Examensarbete
TVVR 13/5004

A numerical simulation of the shape of submerged breakwater to minimize mean water level rise and wave transmission

Takahiro Uemura

Division of Water Resources Engineering
Department of Building and Environmental Technology
Lund University

Avd för Teknisk Vattenresurslära
TVVR-13/5004
ISSN 1101-9824

A numerical simulation of the shape of submerged breakwater to minimize mean water level rise and wave transmission

Takahiro Uemura

Abstract

It has been widely reported that coastal erosion causes problems worldwide. In order to solve these problems, breakwaters have been constructed in such regions. However, it is also a fact that breakwaters adversely affect the environment and scenery. To be able to prevent coastal erosion, while still preserving the environment and the view, submerged breakwaters have been introduced. However, submerged breakwaters have been shown to have a major flaw: they tend to increase the mean water level behind the breakwater, which in turn is a factor causing further erosion of the coast. One example of such a scenario is the west coast of Niigata, Japan. In order to minimize this mean water level rise, a number of studies have been carried out, but most of them do not reduce either the mean water level or the wave transmission sufficiently. Therefore, this paper aims to develop the shape of the submerged bank to minimize both the mean water level rise and the wave transmission. A numerical calculation in two dimensions has been carried out under the assumption that the submerged bank is of great length. Calculations are done for both submerged banks modeled after existing banks in Niigata, and for long, low submerged banks with several vertical impermeable plates. The obtained results were compared to each other in regards of spectrum analysis, mean water level, significant wave heights behind the bank, and significant wave height in long waves. The newly-introduced submerged bank showed high efficiency in minimizing the mean water level and wave transmission. Furthermore, the submerged bank could minimize the transmission of long waves, which shows great promise for future implementation.

Table of Contents

1. Introduction ..... - 1 -
1-1. Background ..... - 1 -
1-2. Objective ..... - 4 -
1-3. Procedure ..... - 4 -
1-4. Past Studies ..... - 4 -
2. Numerical Model ..... - 8 -
2-1. CADMAS-SURF ..... - 8 -
2-2. Certainty of CADMAS-SURF ..... - 11 -
3. Cases Studied ..... - 12 -
3-1. Analytic Area ..... - 12 -
3-2. Incident Waves ..... - 16 -
3-3. Cases ..... - 18 -
4. Results and Discussion ..... - 22 -
4-1. Wave Analysis and Mean Water Level Rise ..... - 22 -
4-2. The Correlation of Wave Height and Mean Water Level Rise ..... - 35 -
4-3. Approach to the Reason of Wave Attenuation ..... - 38 -
4-4. Examinations from the Velocity Distributions ..... - 40 -
5. Conclusion ..... - 42 -
Appendix A Incident Waves ..... - 43 -
Appendix B Results of All the Cases ..... - 45 -
B-1. Comparison of the trapezoidal submerged breakwaters ..... - 45 -
B-2. Comparison of the submerged breakwaters with and without vertical plates at the same structure heights ..... - 47 -
B-3. The effect of vertical plates of two different heights ..... - 51 -
B-4. The effects of vertical plates of three different heights ..... - 55 -
B-5. The effects of wave shoring in Case A, A' and D ..... - 57 -
B-6. Wave velocity ..... - 61 -
6. References ..... - 71 -

1. Introduction

1-1. Background

The west coast of Niigata is located on the North-west seaboard of Japan, where the monsoons blow strongly in the direction of South-east in winter (Figure 1-1 and 1-2).

Figure1-1 Winter storm on the west coast of Niigata

(MLIT, 2001)

Figure1-2 Map of Niigata, Japan

According to the wave data measured offshore on the west coast of Niigata, the maximum significant wave height and wave period observed between December 2011 and January 2012 were $T_{1/3}$=5.3m and $H_{1/3}$=11.8s, respectively (Coastal Development Institute of Technology, 2012). Despite such high incident waves, sand from the Shinano river, the longest river in Japan, flowed into the coastal zone and moved the coastal line seaward. However, it has suffered from severe coastal erosion after dams started to be built along the Shinano River. The construction began in the 1870s. The coastal line retreated by an annual average of 5.0 meters between 1912 and 1926, and the total retreat is at 350 meters by now (Ministry of Land, Infrastructure, Transport and Tourism, 2001). In order to minimize the erosion, submerged breakwaters, which are 1,580 meters long, 40 meters wide on its top and 6.5 meters high, were built 500 meters offshore in 1989 (Figure 1-3 and 1-4). Submerged breakwaters were considered appropriate as the tidal variation in the area is 28 cm. This

means that maintaining a constant depth as measured from the sea surface to the top of the bank is fairly easy. As expected, the transmitted waves over the submerged bank have decreased in size. However, the breakwaters have also caused a rise in mean sea levels, leading to the difference in pressure on both sides of the submerged breakwater. The water levels then equalize causing the current to further drive sediment away, that is, stronger erosion. It is reported that scouring, a kind of structural erosion, occurs just behind the bank (Kuriyama et al., 2006). Figure 1-5 shows the net change in sediment amount behind the submerged breakwater over the past 10 years. The annual average outflow from Area 1and 2 is -74,000 m^3/year (CDIT, 2012). Although severe coastal retreat has not been reported yet, the outgoing of the sand itself means that the west coast of Niigata is still in a state of imbalance, and there remain concerns of more severe erosion in the future. In short, it is becoming a vital problem for the local residents.

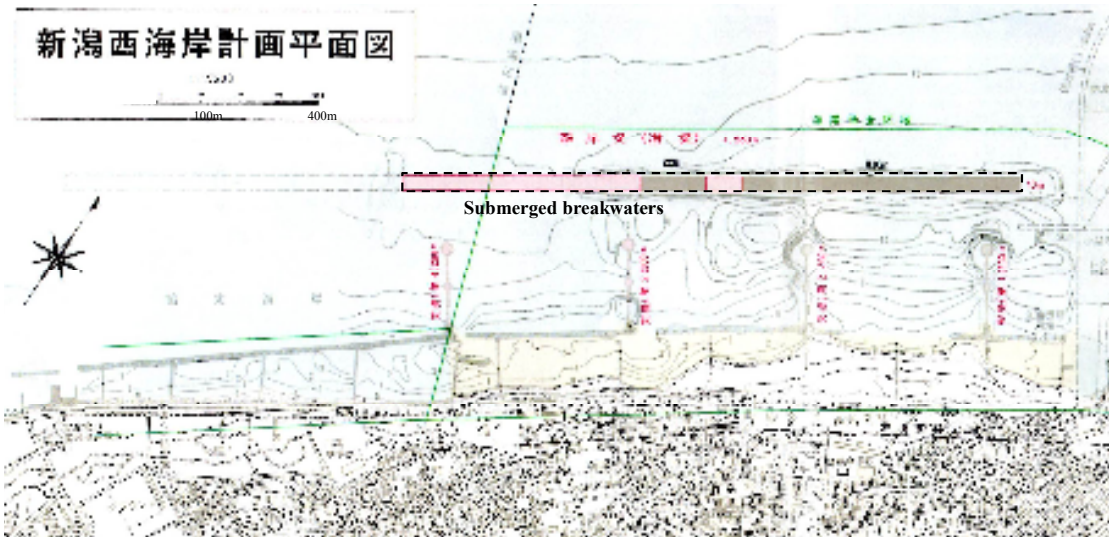

Figure1-3 Plan for the submerged breakwater in Niigata (MLIT, 2001)

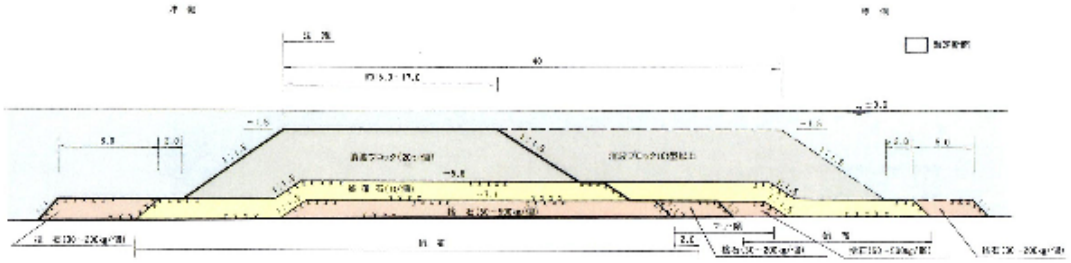

Figure1-4 Cross section of the submerged breakwater in Niigata (MLIT, 2001)

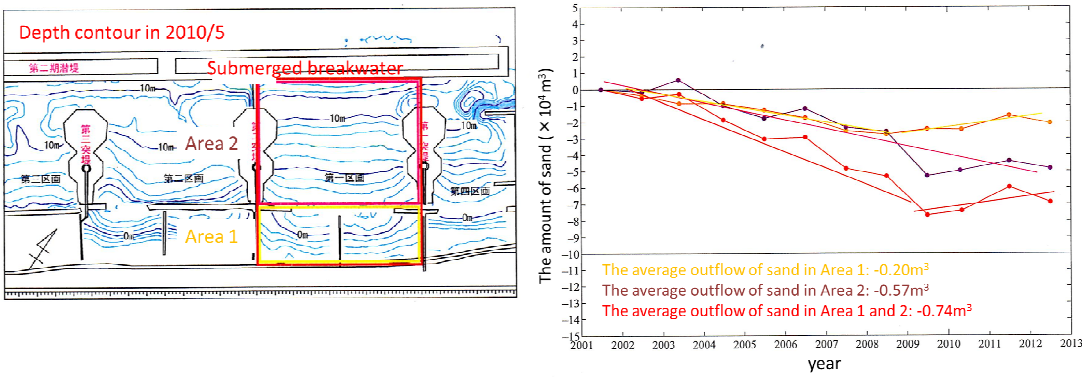

Figure1-5 Average outflow of sand behind the submerged breakwater in Niigata (CDIT, 2012)

1-2. Objective

There should be a lot of regions with the problem of coastal erosions worldwide. Submerged breakwaters might be useful way for wave protection for that kind of area. However, the problem of mean water level rise, which occurred in Niigata, must be avoided there. In order not to lead to it, a developed shape of breakwater is highly needed. This thesis aims to develop a shape of the submerged breakwater in order to minimize both the mean water level rise and wave transmission.

1-3. Procedure

The numerical calculations with CADMAS-SURF, which is widely used in a practice of business in Japan, are two dimensional and are made under the assumption that the submerged breakwater bank is of great length. The similar calculations were carried out for several shapes of submerged breakwaters, and their results address the spacious mean water level along cross-shoreline and transmitted waves behind a submerged breakwater.

1-4. Past Studies

Several studies have been carried out so far in order to solve the problem of mean water level rise caused by submerged breakwaters. According to Fernando et al. (2001), decreasing freeboard yields higher energy flux transmission under nonbreaking conditions (Note that freeboard is negative). K. W. Pilarczyk and R. B. Zeidler (1996) mentioned that enlarging crest width decreases the transmitted waves. On the other hand, J. H Loveless and D. Debski (1998) indicate that the mean water level rise reaches maximum when the height of the breakwater's crest is the same as the sea level, and the water level becomes larger as the crest width becomes wider in a two dimensional experimental study. Calabrese et al. (2003) also conducted large scale experiments in two dimensions. They demonstrated that mean water level rise is dominated by the loss of wave momentum which is connected to wave breakings.

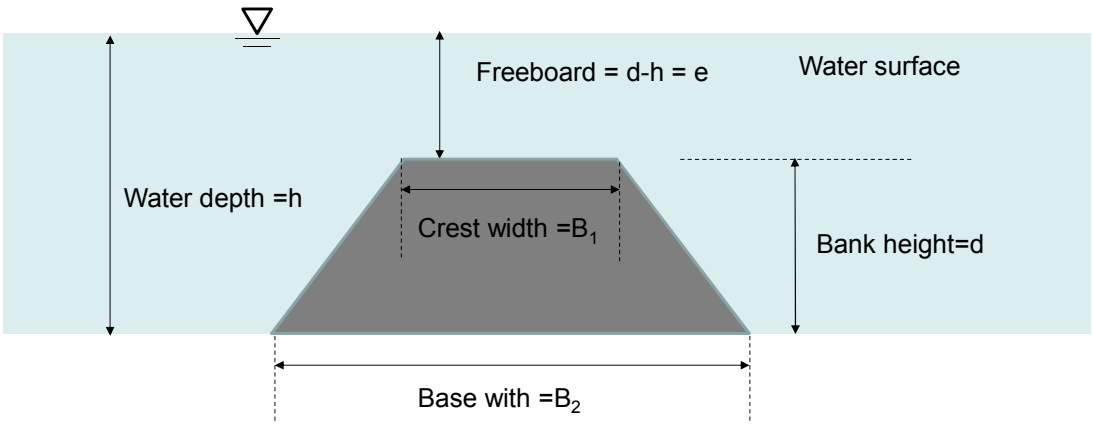

Figure 1-6 The labels for each constituent part of the submerged

1-5. Assumption

As stated above, the objective of this study is to find out a new type of submerged breakwater which can minimize both the mean water level behind the submerged breakwaters and wave transmission simultaneously. The points below were considered in finding a new type of submerged breakwaters in this thesis.

(a) For wave reduction, effective height of submerged breakwater may be necessary since the power of transmitting waves on the top is much greater than on bottom (Figure 1-7).

(b) In order to minimize the mean water level, large wave breaking must be avoided.

Therefore, it might be better if the height of the front part of the submerged breakwater is low.

Thus we have got an assumption that breakwaters with different height horizontally might sufficiently reduce the required condition at the same time. However, we have to take it into consideration that we have to avoid introducing the structures which are difficult to construct. The submerged banks with different top height seem to be difficult to construct from the view point of engineering. According to Yoshida et al. (1988), a submerged-Double-Plate-Breakwater can reduce wave transmission although its effect on mean water level has not been examined. Therefore, we have finally got an assumption that the submerged bank with a couple of vertical impermeable plates might be possible to meet the both (a) and (b) since it is easy to change the plate heights. Figure 1-8 shows the conceptual model of the submerged breakwaters with impermeable plates.

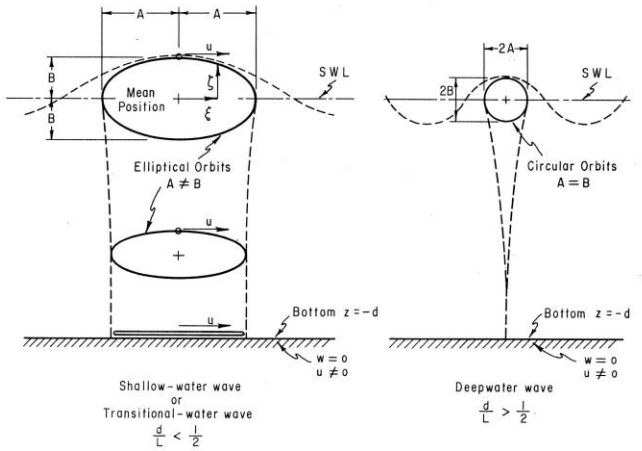

Figure1-7 Movement of a water particle (US Army, 1984)

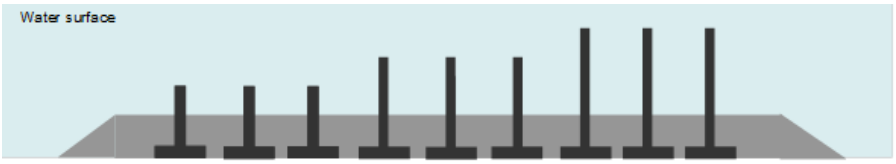

Figure1-8 Conceptual model of the newly-introduced breakwater in this thesis

2. Numerical Model

2-1. CADMAS-SURF

CADMAS-SURF, introduced by Coastal Development Institute of Technology, Japan, 2001, has been adopted into the numerical model in this paper due to the following functions:

- Capable of simulating complex free surfaces.
- High accuracy for describing an obstacle by means of the porous model.
- Capable of locating obstacles/boundaries conditions at any position.
- Several wave-making sources.
- Capable of dealing with bubble contamination as well as water residue.

The *CADMAS-SURF* basically stands upon three basic equations: The continuous equation in two-dimensional incompressible viscous flow (equation 2.1), under the *Porous model*, and the *Navier-Stokes equation* which can be found in equations 2.2 and 2.3.

2.1) Continuity equation

$$\frac{\partial \gamma_x u}{\partial x} + \frac{\partial \gamma_z w}{\partial z} = 0 \quad \text{(Eq. 2.1)}$$

2.2) and 2.3) *Navier-Stokes equation* developed on the basis of the *Porous model*.

$$\lambda_v \frac{\partial u}{\partial t} + \frac{\partial \lambda_x uu}{\partial x} + \frac{\partial \lambda_z wu}{\partial z} = -\frac{\gamma_v}{\rho}\frac{\partial p}{\partial x} + \frac{\partial}{\partial x}\left\{\gamma_x \nu_e \left(2\frac{\partial u}{\partial x}\right)\right\} + \frac{\partial}{\partial z}\left\{\gamma_z \nu_e \left(\frac{\partial u}{\partial z} + \frac{\partial w}{\partial x}\right)\right\} - R_x$$

(Eq. 2.2)

$$\lambda_v \frac{\partial w}{\partial t} + \frac{\partial \lambda_x uw}{\partial x} + \frac{\partial \lambda_z ww}{\partial z} = -\frac{\gamma_v}{\rho}\frac{\partial p}{\partial z} + \frac{\partial}{\partial x}\left\{\gamma_x \nu_e \left(\frac{\partial w}{\partial x} + \frac{\partial u}{\partial z}\right)\right\} + \frac{\partial}{\partial z}\left\{\gamma_z \nu_e \left(2\frac{\partial w}{\partial z}\right)\right\} - R_z - \gamma_v g$$

(Eq.2.3)

where

t is time

x is horizontal coordinate

z is vertical coordinate

u is horizontal velocity of fluid

w is vertical velocity of fluid

ρ is density of water

p is the water pressure

v_e is coefficient of kinematic viscosity, which is summation of molecular kinematic viscosity and eddy

kinematic viscosity

g is the acceleration of gravity

γ_v is porosity

γ_x and γ_z are transmission abilities

$\lambda_v = \gamma_v + (1-\gamma_v)C_M$, $\lambda_x = \gamma_x + (1-\gamma_x)C_M$, $\lambda_z = \gamma_z + (1-\gamma_z)C_M$

where

C_M is a coefficient of inertial force

R_x and R_z are resistance

where

$$R_x = \frac{1}{2}\frac{C_D}{\Delta x}(1-\gamma_x)u\sqrt{u^2+w^2}$$

$$R_z = \frac{1}{2}\frac{C_D}{\Delta z}(1-\gamma_z)w\sqrt{u^2+w^2}$$

where

C_D is resistance

Δx is grid interval of x axis

Δz is the grid interval of z axis

The Volume of Fluid (*VOF*) method (Hirt, 1981) is adopted in order to simulate the free water surface. The advection equation of F on the basis of a porous model can be written as follows (See equation 2.4).

2.4) Advection equation of F, which is a function of *VOF-function*.

$$\gamma_v \frac{\partial F}{\partial t} + \frac{\partial \gamma_x uF}{\partial x} + \frac{\partial \gamma_z wF}{\partial z} = 0 \quad \text{(Eq. 2.4)}$$

In the *VOF method*, the state of each cell, whether the cell is fully saturated with fluid, fully saturated with gas or water surface, can be obtained. Furthermore, the water surface may be fourfold according to the direction of the water surface, which enables us to simulate the free surface of fluid (Figure 2-1). In the decision of the state of the cell, the process mentioned below is repeatedly undone.

① Assume every cell is a saturated cell
② If the cell is $F=0$, it is regarded as a gas cell.
③ The cell of a non-gas cell which is adjacent to a gas cell is regarded as a surface cell.
④ The surface cell which is not adjacent to a saturated cell is regarded as a gas cell.
⑤ Inspecting the cells which are not among saturated cells and gas cells.
⑥ The cells inspected in the procedure ⑤ are changed into gas cells
⑦ Repeating ③-④ until there is no cell which is applicable to ⑤.

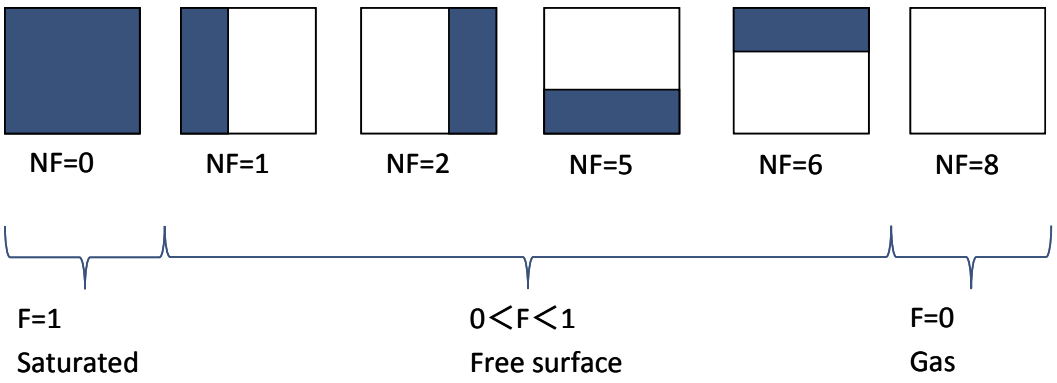

Figure2-1 State of a cell in VOF method

2-2. Certainty of CADMAS-SURF

For the use of the numerical calculation, the certainty of the software is of key importance for the accuracy of the results. As mentioned above, CADMAS-SURF is software which can simulate the waves with very complex free surface. This is also used for the calculation related to transmitted waves behind submerged breakwaters. For instance, Nakagawa et al. (2011) carried out both the three dimensional model tests and two dimensional calculations with CADMAS-SURF. From the obtained results, they concluded that the trends of transmitted waves are similar. For another example, Hieua, P and Tanimoto, K (2006) conducted the numerical calculations with CADMAS-SURF in order to verify its applicability. The research was focused on wave-breaking on slope bottom and wave-breaking over submerged breakwaters. The obtained results of water surface elevations along cross-shoreline distance were compared to experimental results, which showed high accuracy. CADMAS-SURF is thus considered to be applicable to this study as well.

3. Cases Studied

3-1. Analytic Area

Figure 3-1 shows the analytic area of the numerical study where the Niigata west coast is modeled under the decision of each value, although the purpose of this study is to find out the qualitative trend. The *x*-axis and *z*-axis of the domain is *1,000m* and *15.0m* respectively. There is an impermeable slope of 1:20 behind the submerged breakwater, which represents the breaker zone. The water depth is 8m except for the place with the submerged bank and sloping bottom, and the position of the wave source is $x=250m$, and the domain between $x=0m$ and $x=200m$ is a decay area. The waves reflects on the left side without the decay area, and this value has been decided for the reason decay area of longer than two wave-lengths are recommended in the instruction book of CADMAS-SURF and wave length is considered to be approximately 80m in this study. Boundary condition of the left side is open boundary, where waves can pass through without reflection. The waves are almost diminished with simultaneous use of both the open boundary and decay area. The center of the submerged breakwater is located at $x=550m$ in every case, and this position has been decided because the distance of three wave-lengths are needed between the wave between the wave source and the submerged breakwater.

According to the instruction book of CADMAS-SURF, the grid size of *x*-axis is recommended to be shorter than L/80-L/800 where L is the wave length, and $\Delta x:\Delta z$ is recommended to be 1:1-5:1. In this study, changeable grid system is adopted to the *x*-axis in order to meet the condition that enables both high calculation speed and accuracy of the numerical calculation: The grid size of *x*-axis is: $\Delta x=1.0m$ between $x=0m$ and $x=400m$, $\Delta x=1.0$-$0.5m$ in geometric progression between $x=400$ and $x=425$, $\Delta x=0.5m$ between $x=425$ and $x=675$, increase between $\Delta x=0.5$-$1.0m$ between $x=675$ and $x=700$, and $\Delta x=1.0m$ between $x=700m$ to $x=1000m$. The grid size of *z*-axis is a strictly set value that cannot be changed, the size of which is $\Delta z=0.25$. Irregular waves of *Bretschneider-Mitsuyasu Spectrum proposed by Goda* is adopted (OCDI, 2002), and this study has been carried out under the condition of incident waves of $H_{1/3}=3.0m$, $T_{1/3}=10.0$ (See Apendix1). The fluid of this study is viscous fluid (the coefficient of kinematic viscosity is 1.0×10^{-6}, which is considered as a standard value for water. The *Porous model* is, as required, used for the submerged breakwater, it is set as *0.5* at any case. Resistance

coefficient and inertia coefficient are *1.0* and *1.2*, respectively because these values are used in the past study related to the submerged breakwater in Niigata (Nakagawa et al. 2011). The value of each parameter in this study is summarized in Table 3-1 (See the next page). Calculation was carried out over *1500s* for each case because time period of more than 100 waves is considered to be required at least, and the water depth outputs for the total points were *87* along the water (Table 3-2). After the calculation, spectrum, mean water level and relative height behind the submerged bank were analyzed by means of this water-depth data.

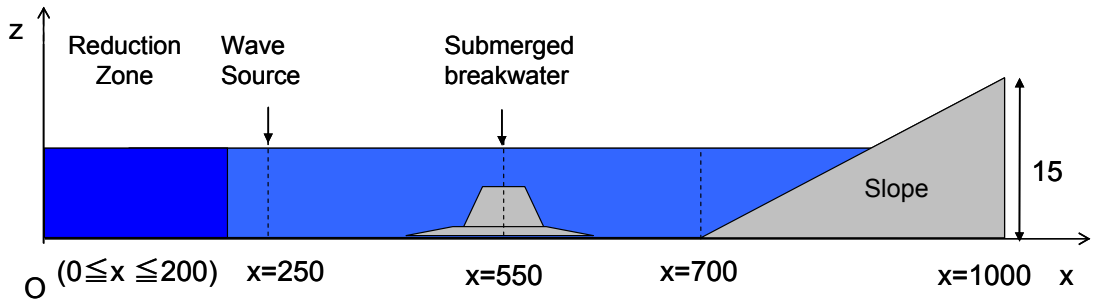

Figure3-1 Cross-section of the analysis domain

Table 3-1 Parameters in the model

Parameter	Value
Length *L(m)*	*1000*
Height *H(m)*	*15*
Grid size *Δx(m)*	*0.5-1.0*
Grid size *Δz(m)*	*0.25*
Source position*(m)*	*250*
Wave-making Function	*Matrix*
Boundary condition of the left side	*Open*
Decay area (*m*)	$0 \leqq x \leqq 200$
Porosity	*0.5*
Inertia coefficient C_M	*1.2*
Resistance coefficient C_V	*1.0*
Kinematic viscosity(m^2/s)	1.0×10^{-6}
Water depth *h(m)*	*8.0*
Significant wave period $T_{1/3(s)}$	*10.0*
Significant wave height $H_{1/3(s)}$	*3.0*
Calculation time (s)	*1500*

Table 3-2 Positions of water depth outputs

Station Number	x (m)	Station Number	x (m)	Station Number	x (m)	Station Number	x (m)	Station Number	x (m)
1	300	21	460	41	560	61	660	81	840
2	310	22	465	42	565	62	665	82	850
3	320	23	470	43	570	63	670	83	860
4	330	24	475	44	575	64	675	84	870
5	340	25	480	45	580	65	680	85	880
6	350	26	485	46	585	66	690	86	890
7	360	27	490	47	590	67	700	87	900
8	370	28	495	48	595	68	710		
9	380	29	500	49	600	69	720		
10	390	30	505	50	605	70	730		
11	400	31	510	51	610	71	740		
12	410	32	515	52	615	72	750		
13	420	33	520	53	620	73	760		
14	425	34	525	54	625	74	770		
15	430	35	530	55	630	75	780		
16	435	36	535	56	635	76	790		
17	440	37	540	57	640	77	800		
18	445	38	545	58	645	78	810		
19	450	39	550	59	650	79	820		
20	455	40	555	60	655	80	830		

3-2. Incident Waves

Incident waves with large wave heights are considered to be suitable for this study because the wave heights, where there are problems of coastal erosions, are normally high. However, the maximum height of waves travelling over the submerged breakwater is limited by the depth of water channel. Irregular waves of Bretschneider-Mitsuyasu spectrum proposed by Goda, at a height $H_{1/3}$=3m, and a period $T_{1/3}$=10.0s has been adapted to incident waves since higher waves easily break before reaching the position of submerged breakwater at x=550m (See the eq.3.1). The process of generating water level height series is as follows.

1. Set the spectrum of the incident waves
2. Divide the spectrum into 500 components based on frequencies
3. Decide the frequency and ample of each frequency-based component
4. Set the phases of each frequency-based component in random numbers.
5. Superimpose all the frequency-based components
6. Calculate water depth and water velocity series from the obtained results in process 5.

The figure shows the spectrum of the incident waves at x=550m, which have been obtained after several calibrations. These same incident waves have been used for every case of the simulation through this study (See the Appendix 1).

3.1) Bretschneider-Mitsuyasu spectrum proposed by Goda

$$S(f) = 0.205 H_{1/3}^2 T_{1/3}^{-4} f^{-5} \exp\left[-0.75\left(T_{1/3} f\right)^{-4}\right] \quad \text{(Eq.3.1)}$$

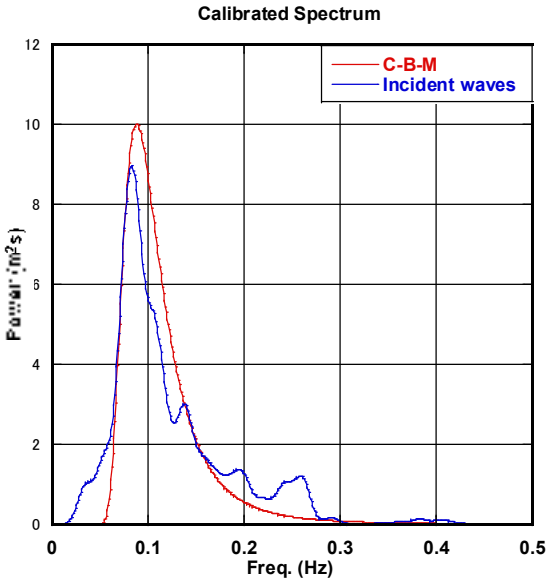

Figure3-2 Spectrum of the incident waves with a height of 3m

3-3. Cases

The cases examined in this study are Cases A and A', trapezoidal submerged breakwaters modeled after the existing bank in Niigata, and Cases B, C and D, which are low submerged banks with several vertical impermeable plates.

Case A

Case A is a trapezoidal submerged bank modeled after the submerged bank in Niigata (Figure 3-3). It is 6.5 meters high (Freeboard e= -1.5m), 40 meters wide on the top of the bank, and 75 meters wide on the bottom of the bank. It consists of two layers of differing permeability. The bottom layer is made of stone, which is considered to be impermeable. The top layer, covering the stone layer, is a tetrapod-with the permeability 0.5.The efficacy of the other bank types discussed later can be measured in comparison to A.

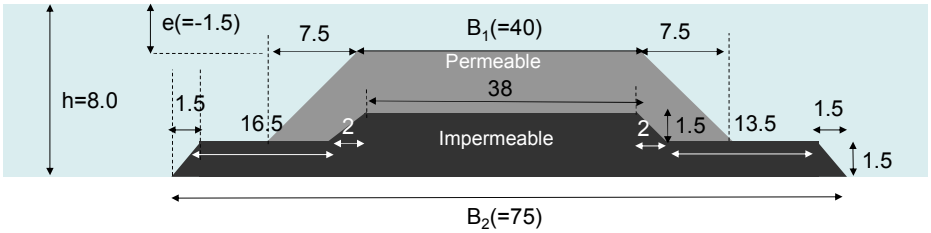

Figure3-3 Cross section of Case A (Trapezoidal submerged breakwater)

Case A'

Case A' is a trapezoidal submerged bank which differs from that in Niigata only in size (Figure 3-4). It is wider and lower than A, the original submerged bank. It is 80 meter wide on the top of the bank (twice as wide as A), and 111 meters wide on the bottom of the bank. Three different heights were tested in this model, namely: 5 meters (e= -3.0m), 5.5 meters (e= -2.5m) and 6.0 meters (e= -2m)

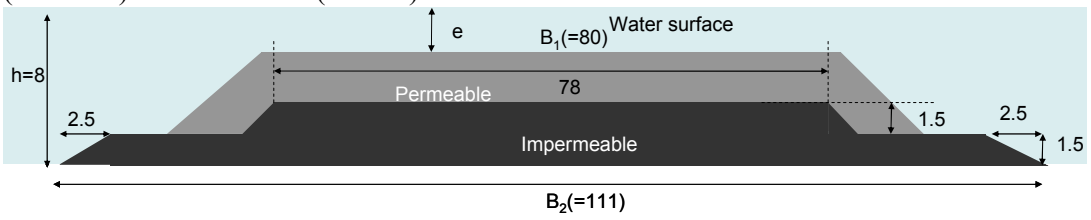

Figure3-4 Cross-section of Case A' (Low, wide trapezoidal submerged breakwater)

Case B

Case B is a low, trapezoidal submerged breakwater with vertical impermeable plates of the same height (Figure 3-5). Although T-blocks were used instead of vertical plates, the hydraulic features of T-blocks are treated as the same as those of vertical plates (Figure 3-6). The height of the impermeable, trapezoid part is 3 meters, almost half of A. Three different widths (B_2=71m, 91m and 111m (n_1=5, 7 and 9)) were also tested. e= -3m, -2.5m -2.0m were undone, which allows us to pinpoint the effect caused by the different widths/plate-heights. Compared to Case A or A', the difference in effects with or without vertical plates can be examined.

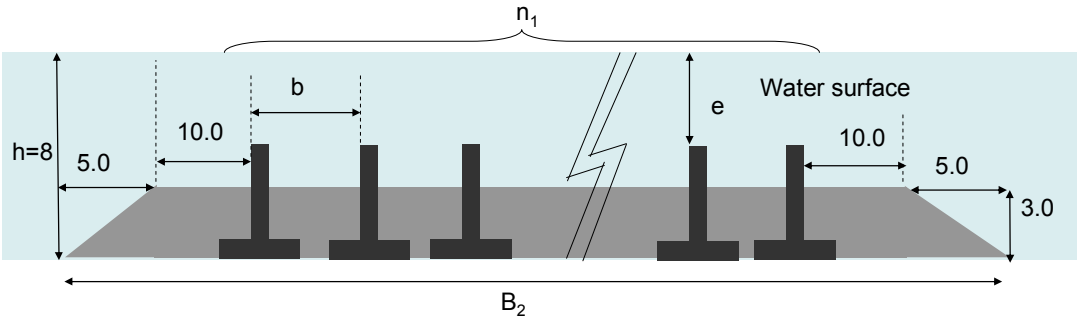

Figure3-5 Cross-section of Case B (Submerged water with vertical plates)

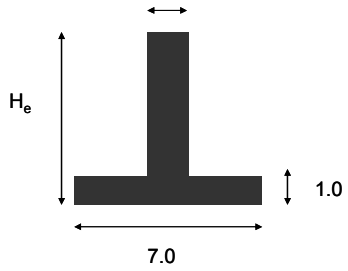

Figure3-6 T-block

Case C

Case C is a low, trapezoidal submerged breakwater with vertical impermeable plates of two different heights (Figure 3-7). The height of the plates in the back part of the bank is higher than the plates in the front part by 0.5 meters: e= -3.0m to -2.5m, e= -2.5m- to -2.0m and e= -2.0m to -1.5m. Otherwise, the shape is the same as in Case B. By comparing the results with B (to be discussed later), we can examine the differences in terms of effect when changing the height of the impermeable plates.

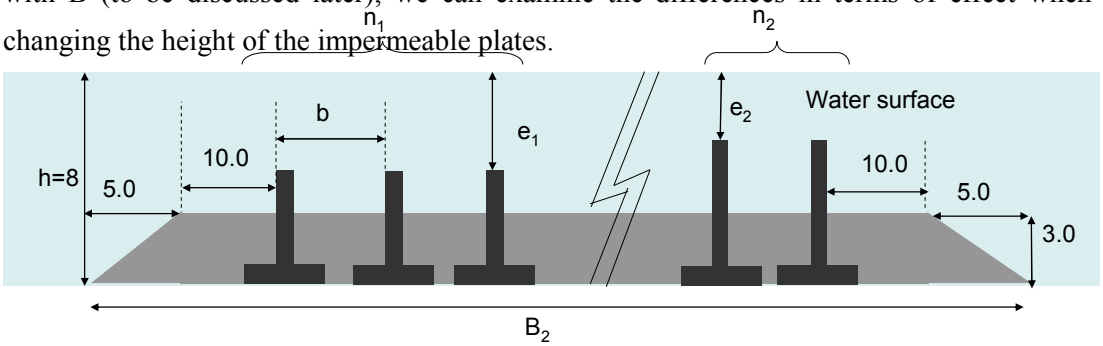

Figure3-7 Cross-section of Case C (Submerged breakwater with plates of two different heights)

Case D

Case D is a low trapezoidal submerged breakwater with vertical impermeable plates of three different heights (Figure 3-8). The height of the plates in the middle part of the bank is set higher than the plates in the front part by 0.5 meters, and the height of the pates in the back part is higher than the middle part by 0.5 meters: e= -3.0, -2.5 and -2.0m, e= -2.5, -2.0 and -1.5m. This Case D was carried out just for the cases in 111 meter wide (n=9). The shape is same as B and C. It is possible to study the differences in effect due to gradually changing the height of the plates by comparing with B.

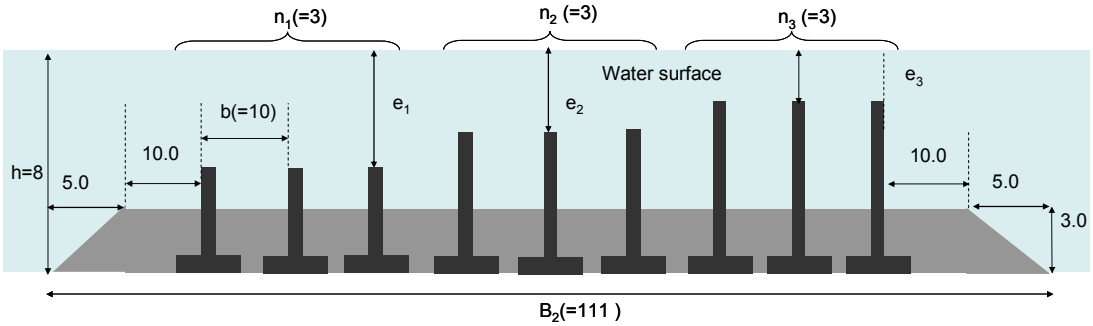

Figure3-8 Cross-section of Case D (Submerged breakwater with plates of three different heights)

All the cases carried out here are summarized in Table 3-3 to 3-6

Table 3-3 Parameter in Case A and A'

Case name	e	B_2
Case A	2.5	75
Case A'3.0	3.0	111
Case A'2.5	2.5	111
Case A'2.0	2.0	111

Table 3-4 Parameter in Case B and C (n=5)

Case name	e_1	e_2	n_1	n_2	B_2
Case B3.0	3.0	-	5	-	71
Case B2.5	2.5	-	5	-	71
Case B2.0	2.0	-	5	-	71
Case C3.0	3.0	2.5	3	2	71
Case C2.5	2.5	2.0	3	2	71

Table 3-5 Parameter in Case B and C (n=7)

Case name	e_1	e_2	n_1	n_2	B_2
Case B3.0	3.0	-	7	-	91
Case B2.5	2.5	-	7	-	91
Case B2.0	2.0	-	7	-	91
Case C3.0	3.0	2.5	4	3	91
Case C2.5	2.5	2.0	4	3	91

Table 3-6 Parameter in Case B, C and D (n=9)

Case name	e_1	e_2	e_3	n_1	n_2	n_3	B_2
Case B3.0	3.0	-	-	9	-	-	111
Case B2.5	2.5	-	-	9	-	-	111
Case B2.0	2.0	-	-	9	-	-	111
Case C3.0	3.0	2.5	-	5	4	-	111
Case C2.5	2.5	2.0	-	5	4	-	111
Case D3.0	3.0	2.5	2.0	3	3	3	111
Case D2.5	2.5	2.0	1.5	3	3	3	111

4. Results and Discussion

From the numerical calculation, water depths in several points were obtained. Although all the calculations were carried out for 1,500s, the data for the last 1024s will be used here because the data for the first calculation time is before the waves have reached the points of data collection.

4-1. Wave Analysis and Mean Water Level Rise

This section is divided into several parts. First we discuss how the change in width and freeboard affect wave attenuation and sea water level rise, focusing on the trapezoidal submerged breakwaters in Cases A and A'. Next, we discuss the differences between the breakwaters with vertical plates and those without using data from Cases A' and B. In the third section we examine the effect of submerged banks with vertical plates of different heights by comparing Cases B and D. Finally, we compare the most successful trapezoidal and non-trapezoidal models in order to find the most suitable design for submerged banks. Although several models were tested, only the most relevant ones are supplied in this section for the sake of legibility. The rest of the results are given in Appendix 2.

Comparison of the Trapezoidal Submerged Breakwaters

This part summarizes only the cases of trapezoidal submerged breakwaters. Figure 4-1 and Figure 4-2 show the shape of Case A and A'2.0 respectively. Figure 4-3 shows the obtained wave spectrum at x=700m, which is 150m behind the submerged bank, and Figure 4-4 shows the spacious mean water level. From Figure 4-3, the wave power of Case A'2.0 is lower than Case A at almost every frequency, which means Case A' has higher effects on attenuation. The difference in mean water level rise dL in figure 4-4 is used to compare the results since the strongest current occurs when the highest and lowest water levels are equalized. The difference in water level in Case A is 0.30m, and the one in Case A'2.0 is 0.19m, which means Case A' is more effective than Case A from the view of mean water level alone. It can be shown that the wide, low trapezoidal breakwaters tend to minimize them more than the existing trapezoidal submerged breakwaters.

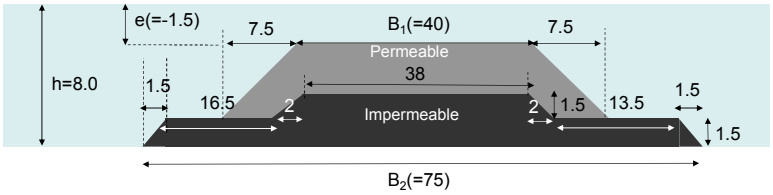

Figure 4-1 Cross section of Case A (Trapezoidal submerged breakwater)

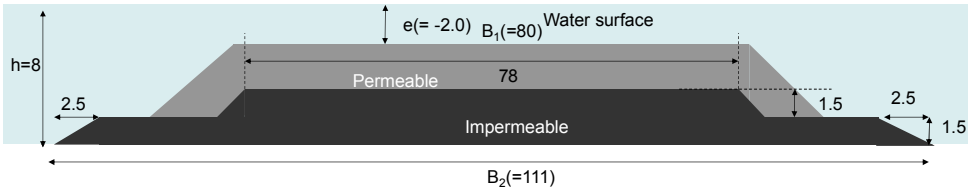

Figure 4-2 Cross section of Case A' (Wide trapezoidal submerged breakwater)

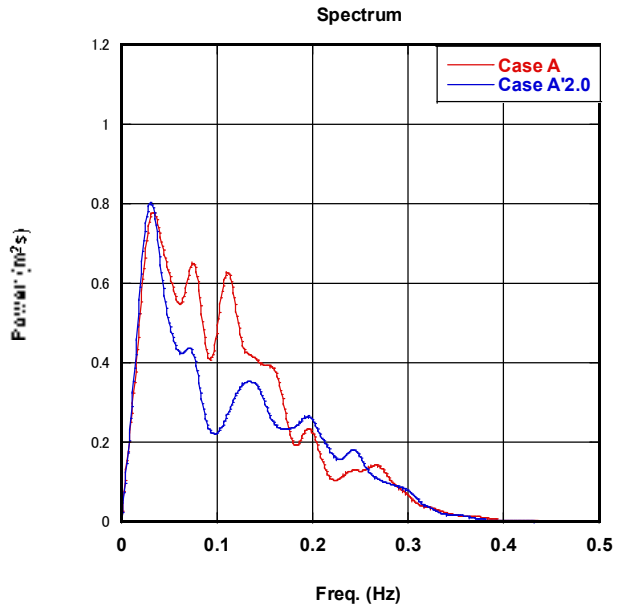

Figure 4-3 Wave spectrum at x=700m in Case A and A'2.0

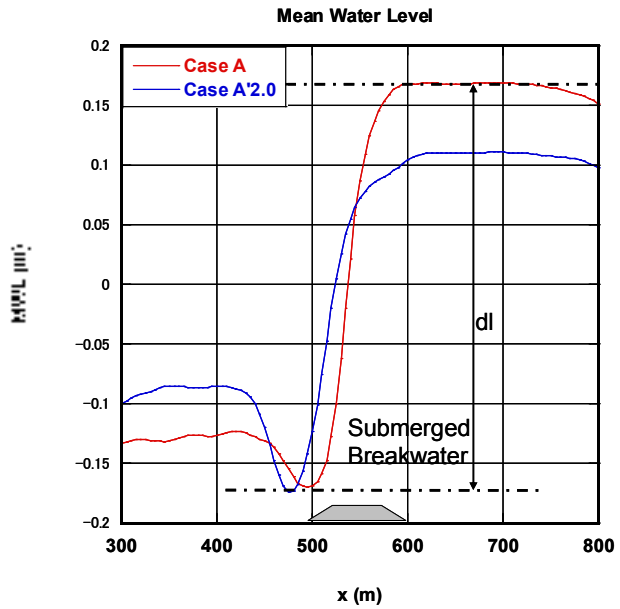

Figure 4-4 Mean water level in Case A and A'2.0

Comparison of the Submerged Breakwaters with and without Vertical Plates at the Same Structure Heights

In this part, we focus on the effects of impermeable vertical plates. Figure 4-5, Figure 4-6 and Figure 4-7 show the shapes of Case A, A'2.0 and B2.0 respectively. Case B, which we will treat here, has nine impermeable vertical plates. The base widths B_2 of Cases A'2.0 and B2.0 are the same. Figure 4-8 shows the wave spectrum at x=700m, obtained at 150m behind the submerged bank, and Figure 4-9 shows the spacious mean water level. From Figure 4-8, the total wave power of B2.0 is almost the same as that of Case A'2.0. It is also notable that the shape of the Case B2.0 wave spectrum is quite different from what we see in A and A'2.0. To wit, the long waves (the waves with low frequency in Case B) are more attenuated. In Figure 3-9, we see that the mean water level rise ΔL is at 0.3m in Case A, 0.19m in Case A'2.0, and 0.26m in Case B2.0. This implies that model B is better than A for preventing mean water level rise, but worse than A'. It can be demonstrated that wide breakwaters with impermeable vertical plates tend to reduce both wave energy and mean water level rise more than the current trapezoidal bank, but also that the most efficient solution is low, trapezoidal banks.

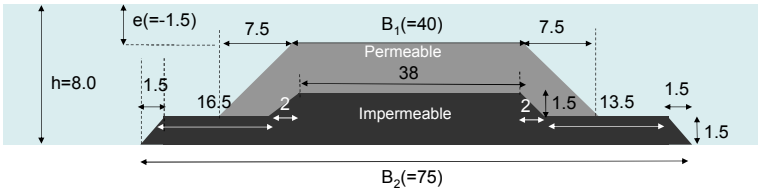

Figure 4-5 Cross section of Case A (Trapezoidal submerged breakwater)

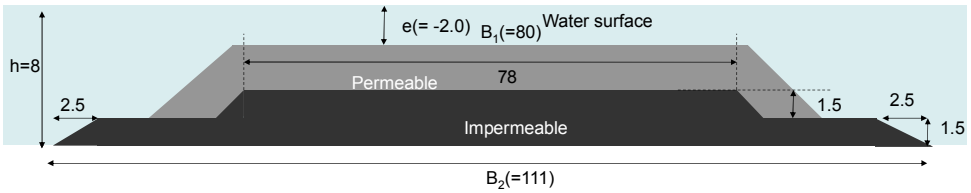

Figure 4-6 Cross section of Case A' (Wide trapezoidal submerged breakwater)

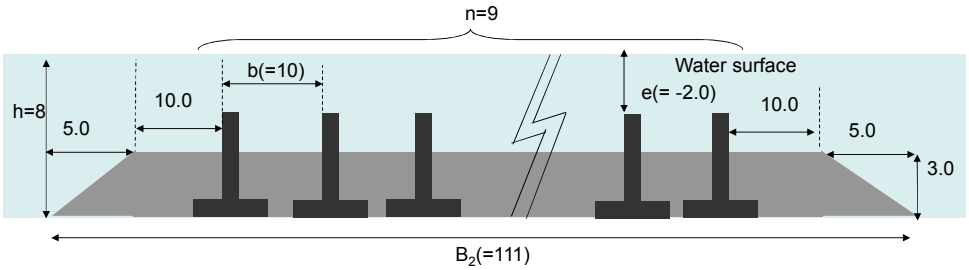

Figure 4-7 Cross-section of Case B (Submerged breakwater with plates)

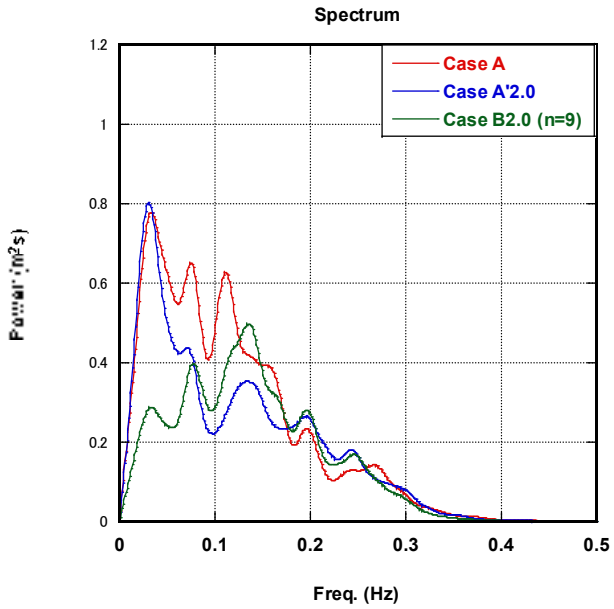

Figure 4-8 Wave spectrum at x=700m in Case A, A'2.0 and B2.0

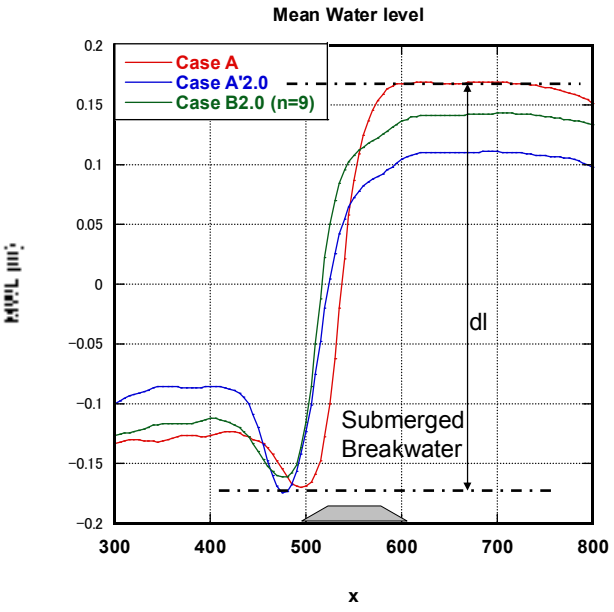

Figure 4-9 Mean water level in Case A, A'2.0 and B2.0

The Effect of Vertical Plates of Different Heights

Now we turn to the question of differing heights in vertical impermeable plates. Cases B2.0 and D2.5 will be treated as representative of trapezoidal submerged breakwaters and submerged breakwaters of three different heights respectively. Figure 4-10, Figure 4-11, and Figure 4-12 show the shapes of Cases A, B2.0, and D2.5, in that order. B and D have nine impermeable vertical plates each, and the same width as B_2. Figure 4-13 gives the obtained spectrum at x=700m, which is 150m behind the submerged bank. Figure 4-14 shows the spacious mean water level. From Figure 4-13, it becomes clear that the wave powers in B2.0 and D2.5 are smaller than in A. In other words, the long, low-frequency waves in B are more attenuated than in A. Furthermore, we can see in Figure 4-14 that the mean water level rise dl in A is 0.3m, 0.25m in B2.0, and 0.17m in D2.5. This implies that Case D is more successful at reducing mean water level rise than either A or B. We can therefore conclude that D, the submerged breakwater with impermeable vertical plates with different heights, is the most useful model for minimizing wave transmission as well as rising water levels.

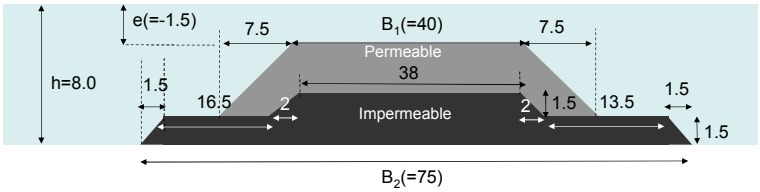

Figure 4-10 Cross section of Case A (Trapezoidal submerged breakwater)

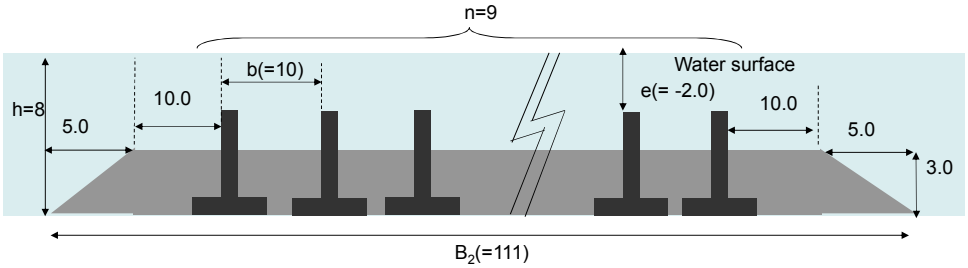

Figure 4-11 Cross-section of Case B (Submerged breakwater with plates)

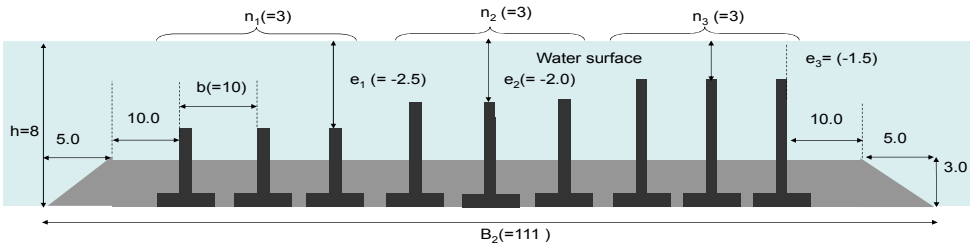

Figure 4-12 Cross-section of Case D (Submerged breakwater with plates of three different heights)

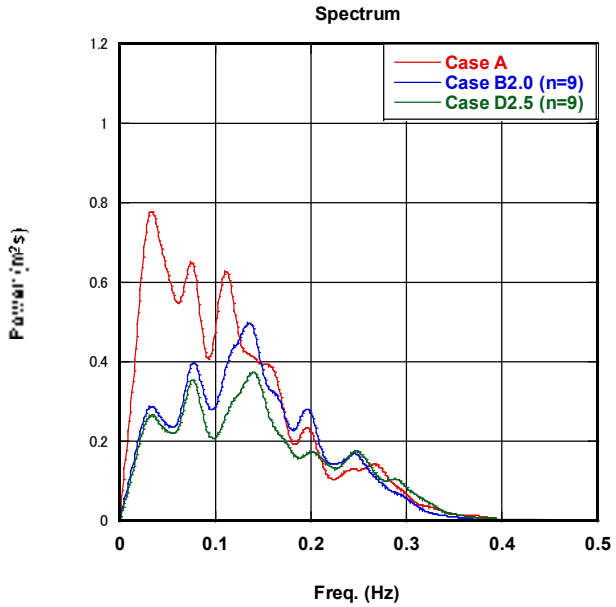

Figure 4-13 Wave spectrum at x=700m in Case A, B2.0 and B2.5

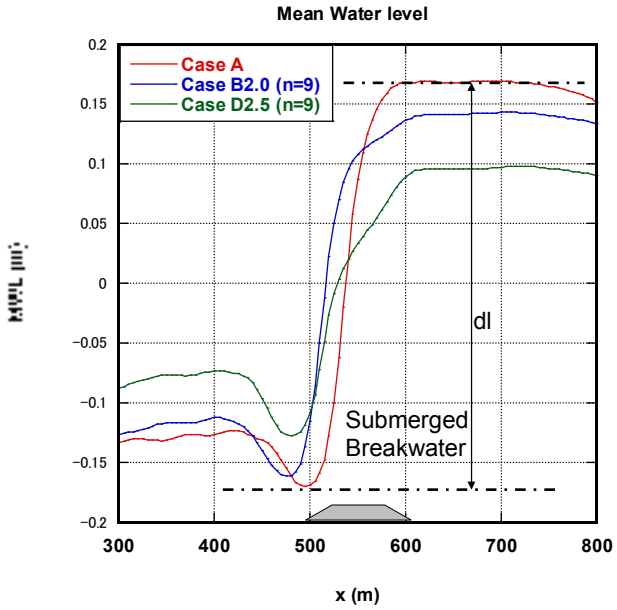

Figure 4-14 Mean water level in Case A, B2.0 and D2.5

Comparison of the Best Cases

This part contains a summary of the cases which have been identified in this chapter as sufficiently effective models for submerged breakwaters. Case A'2.0 has shown to be the most effective trapezoidal submerged breakwater in this study. Case D2.5 is the most effective submerged breakwater with vertical plates. Case D3.0 is also discussed since Case D seems to be one of the most efficient bank designs in this study. Figure 4-15, 4-16. 4-17 and 4-18 show the shape of Case A, A'2.0, D3.0 and D2.5 respectively. Figure 4-19 shows the obtained wave spectrum at x=700m, which is 150m behind the submerged bank, and Figure 4-20 shows the spacious mean water level. From Figure 4-19, the wave power of Case D2.5 is lowest of all. Both Case D3.0 and Case D2.5 clearly reduce the energy of long waves. From Figure, the mean water level rise dL in Case A, A'2.0, D3.0 and D2.5 is 0.30m, 0.19m, 0.08m, 0.17m, respectively. The mean water level rises in Case D are lower than the others. In conclusion, it can be shown that the breakwaters with vertical impermeable plates can minimize them more than the existing trapezoidal submerged breakwaters and low, wide trapezoidal banks.

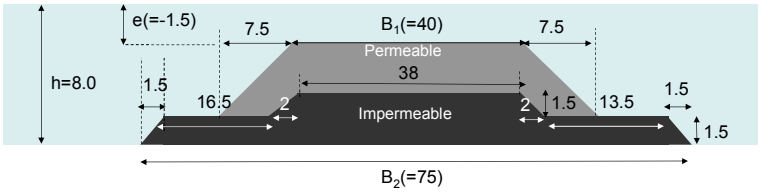

Figure 4-15 Cross section of Case A (Trapezoid submerged breakwater)

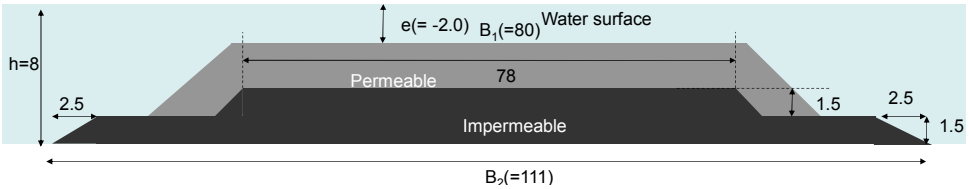

Figure 4-16 Cross section of Case A' (Wide trapezoid submerged breakwater)

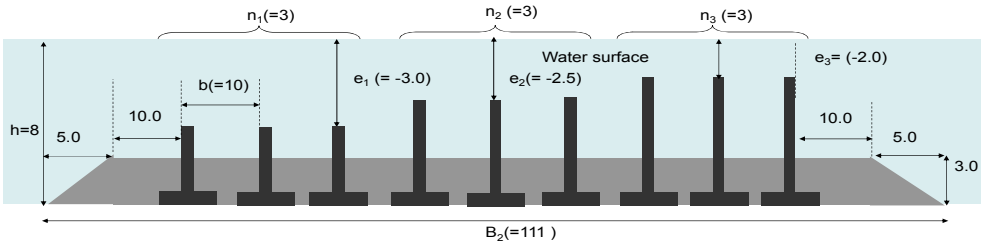

Figure 4-17. Cross-section of Case D2.5 (Submerged breakwater with plates of three different heights)

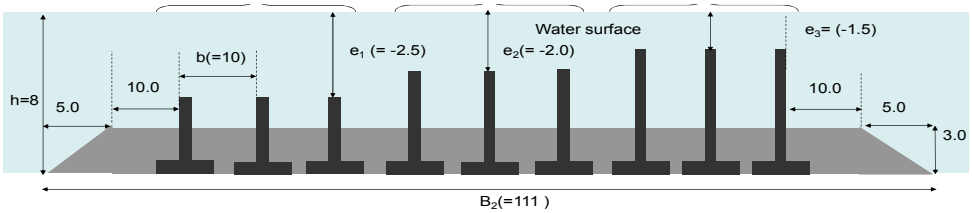

Figure 4-18. Cross-section of Case D2.0 (Submerged breakwater with plates of three different heights)

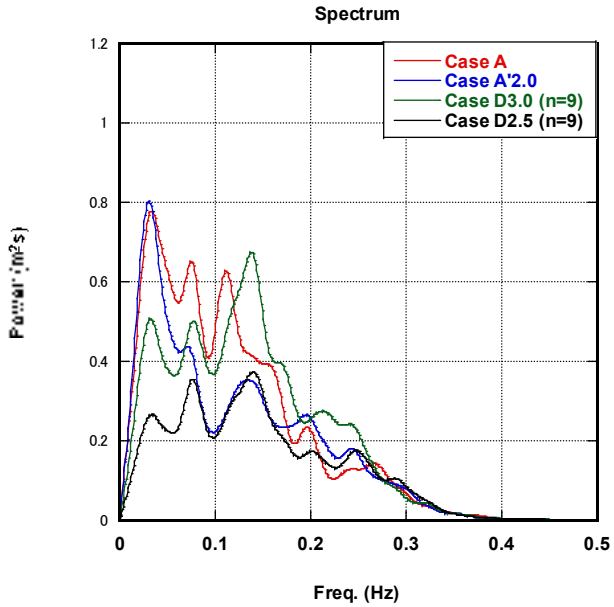

Figure 4-19 Wave spectrum at x=700m in Case A, A'2.0, D3.0 and D2.5

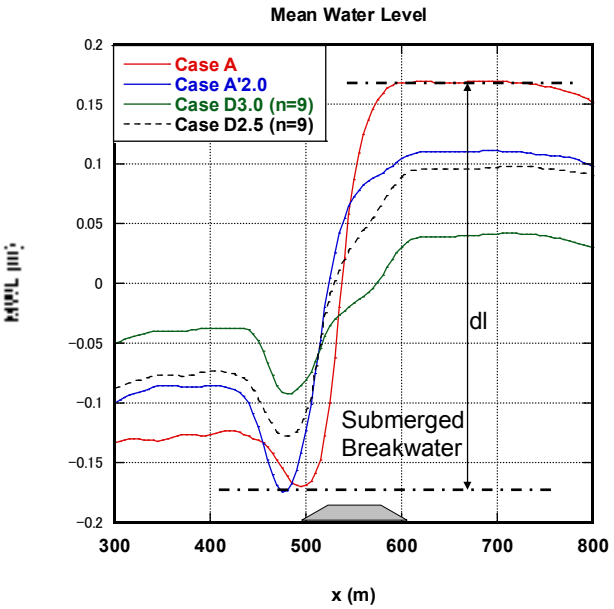

Figure 4-20 Mean water level in Case A, A'2.0, D3.0 and D2.5

The Effect of Wave Shoaling

As the waves approach the shoreline, they tend to become higher. Figure 4-21 and Figure 4-22 show the wave spectrum at x=700 of the trapezoidal submerged bank and submerged banks with the vertical plates of different heights. From the two figures below it can be inferred that Case D reduces long waves drastically at the place near the shoreline, as compared to A and

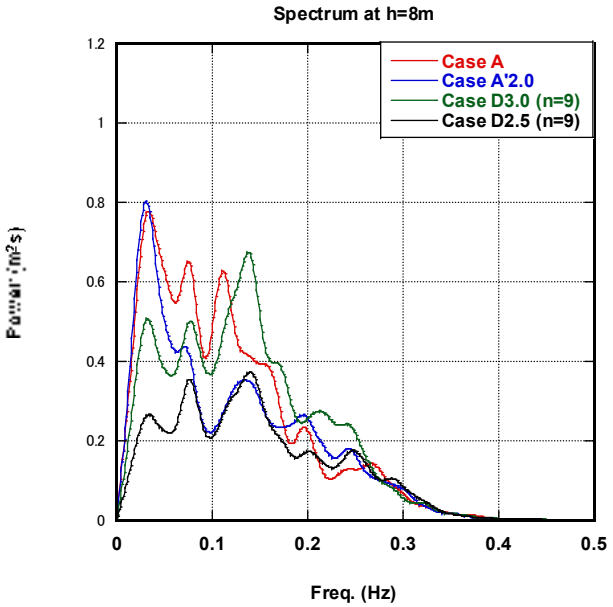

Figure 4-21 Wave spectrum at x=700m in Case A, A'2.0, D3.0 and D2.5

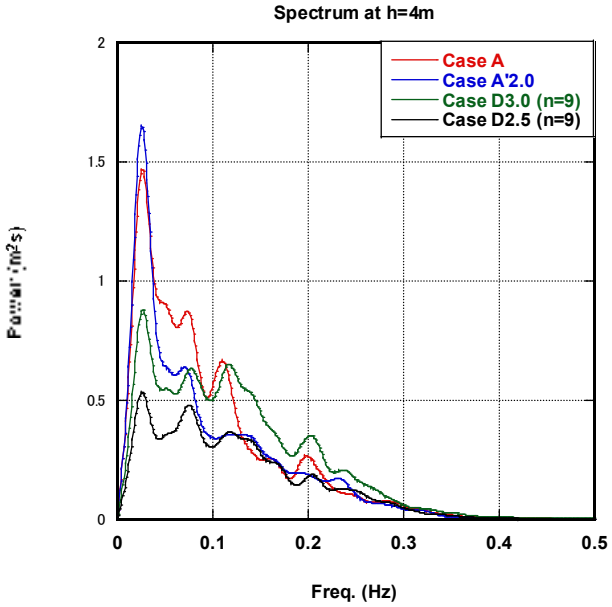

Figure 4-22 Wave spectrum at x=780m in Case A, A'2.0, D3.0 and D2.5

4-2. The Correlation of Wave Height and Mean Water Level Rise

Section 4-1 has successfully demonstrated that the submerged breakwaters with vertical plates are more suitable through spectrum and mean water level analysis. Nevertheless, it can be hard to predict the efficiency of a model from just the wave spectrum. In this section, the wave spectrums of all the cases are converted into wave heights and discussed from different angles.

- The correlation of Significant wave height and Mean Water Level Rise.
- The correlation of the equivalent long-wave height.

The Correlation of Significant Wave Height and Mean Water Level Rise

Significant wave heights have been obtained by zero-upcrossing method at a certain point, which is here set at x=700m. The Figure 4-23 shows the correlation diagram of the significant wave and mean water level rise in each case. The red point, blue square, green triangle and black circle define the trapezoidal submerged breakwaters, and the submerged breakwaters with five, seven and nine vertical plates respectively. The lower the point is located, the lower the difference in mean water level becomes. The more left the point located, the lower the significant waves behind the submerged banks become. Therefore, the cases located in the low-left area, namely the area surrounded by the red broken-line in the figure, are considered as the most preferable cases, which can reduce both wave transmission and mean water level rise. Thus, Case D3.0, D2.5, C2.5 and C3.0, the submerged banks with vertical plates of three/two different heights, are regarded as the most preferable shape.

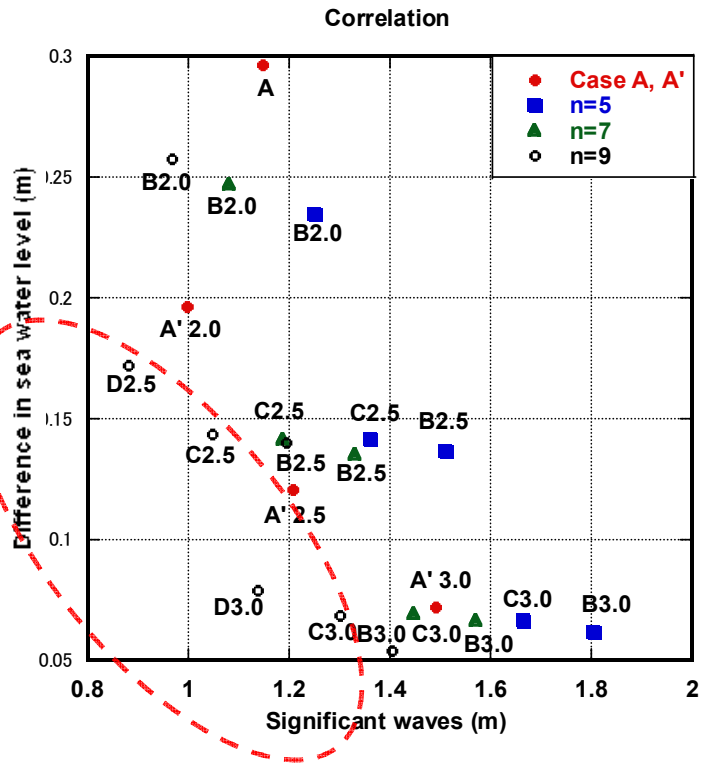

Figure 4-23 Correlation diagram between significant heights and mean water levels

The Correlation of the Equivalent Long-wave Height and Mean Water Level

In the section 4-1, it has been shown that the newly-introduced submerged breakwater, the breakwater with vertical plates, is remarkably effective on long-waves. This section discusses in more detail the long-wave components of the wave transmission. The long waves here are defined as waves with longer periods than 10s, that is, lower frequencies than 0.1Hz. The concept of equivalent long-wave heights has been adopted in this examination. The equation 4.1 and Figure 4-24 contain the definition of equivalent long-wave height. The coefficient C is assumed as 4.0 here. However, the value of coefficient should not affect the comparison (What is larger among the cases should be same).

$$H_L = C\sqrt{S_L} \quad \text{(Eq.4.1)}$$

where

H_L: Equivalent long-wave height

C: Coefficient

S_L:The total area of S_L in Figure 3-24

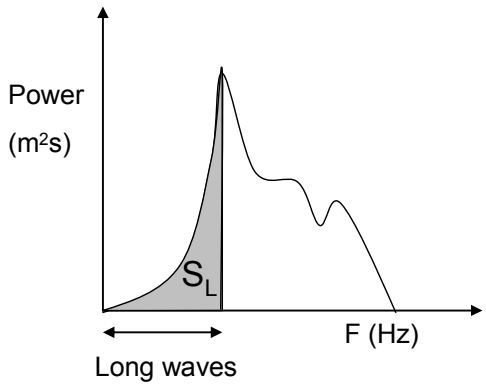

Figure 4-24 Definition of S_L in eq.3.1

Figure 4-25 shows the correlation diagram of the equivalent long-wave height at x=700m and mean water level rise in each case. The lower the point is located, the lower the difference in mean water level becomes. The more left the point located, the lower equivalent long-wave height behind the submerged bank is. Thus, the cases located in the low-left area, namely the area surrounded by the red broken-line in the figure, are able to minimize both long-wave transmission and mean water level rise. As can be seen, in most of the Cases in B, C and D, submerged breakwaters with vertical plates are more appropriate for reducing long-waves and mean water levels in comparison to the trapezoidal submerged breakwaters. Notably, Case D exhibits a decrease in both.

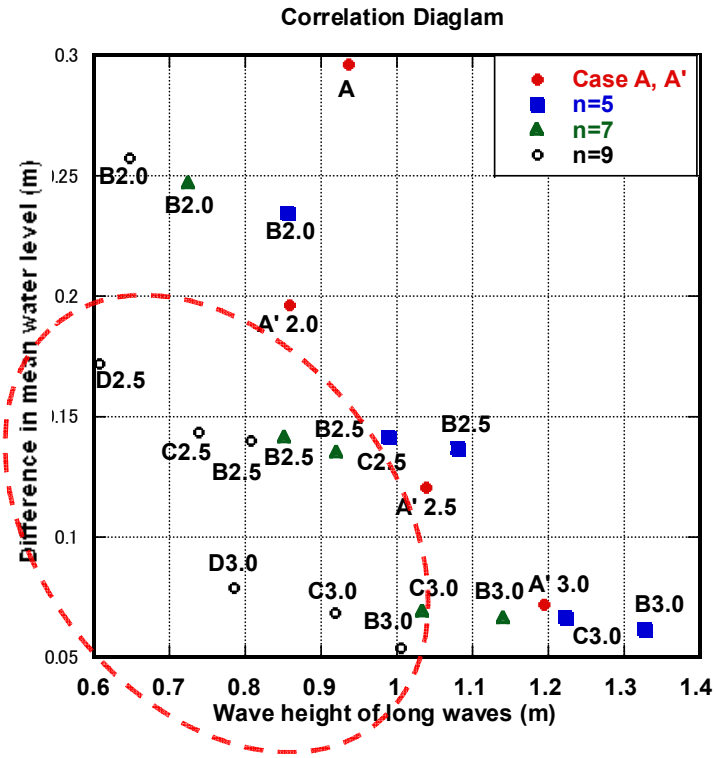

Figure 4-25 Correlation Diagram between wave heights of long waves and mean water levels

4-3. Approach to the Reason of Wave Attenuation

Examinations for Wave Reflection

This section examines the reasons for wave attenuation behind the submerged breakwaters in order to examine the following assumption.

- At first we thought that the higher rate of success at reducing wave transmission observed in the newly introduced submerged breakwater was due to a greater degree of reflection.

Figure 4-26 shows the spectrum of incident waves and reflected waves at x=350m, that is, 200m offshore from the submerged bank. If the energy of the reflected waves in Case D is bigger than in Case A, it can be surmised that the reflection has caused a decrease in energy behind the submerged bank in D. However, the difference in energy between A and D is in reality quite small. The reflection by the submerged breakwater with the vertical plates is not larger than that of the trapezoidal bank. Therefore, it can be concluded that the wave energy in D must have decreased over the submerged breakwater for another reason.

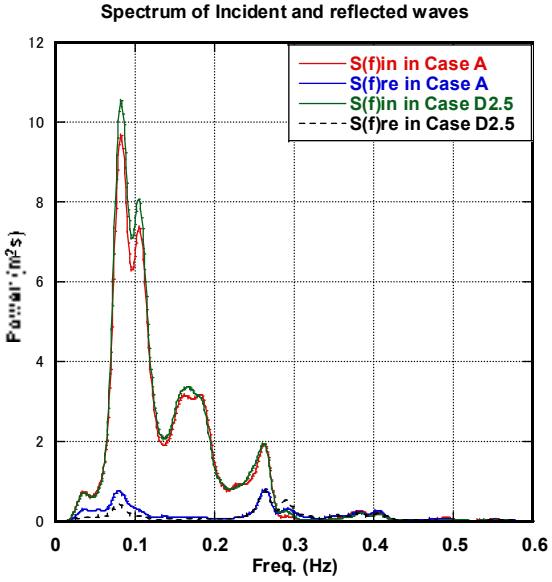

Figure 4-26 Spectrums of incident waves and reflected waves at x=350m

4-4. Examinations from the Velocity Distributions

Figure 4-27 and 4-28 show the velocity distributions at a certain time in Case A and D respectively. Although the waves seem to transmit as a surge in Case A, the waves in Case D appear to pass over the submerged bank relatively smoothly. In addition, in Case D, more vortexes seem to be generated than in Case A. The energy of incident waves in Case D might have been reduced because of these vortexes.

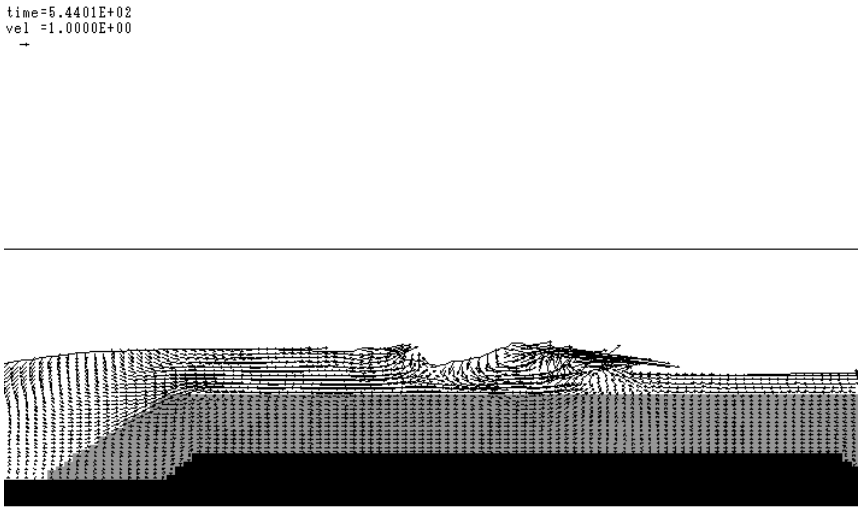

Figure 4- 27 Wave velocity distributions in Case A (Trapezoidal submerged breakwater)

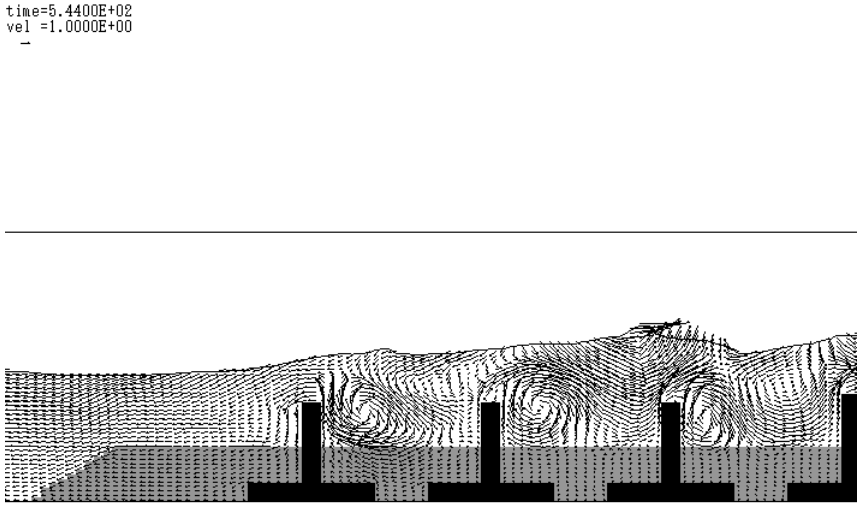

Figure 4- 28 Wave velocity distributions in Case D (Newly-introduced submerged bank)

5. Conclusion

The aim of this paper was to develop the shape of a submerged breakwater bank in order to minimize both the mean water level rise and wave transmission. The two dimensional numerical calculations point toward the efficacy of wide and low submerged breakwaters with several vertical impermeable plates of differing heights, in order to achieve these goals. They showed the breakwaters with vertical plates of more gradually-changed heights have more efficiency. They also proved to be remarkably efficient for the attenuation of long waves. Although submerged breakwaters of this kind would be wider than the banks already in place in Niigata, they are feasible because the low height requires a much smaller volume of construction materials. Additionally, they would also be fairly easy to build since their constituent parts are not comprised of complex shapes. This proposal for the design of submerged breakwaters is preliminary. Although the aspects focused on in this paper were only the power of transmitted waves, wave heights behind the submerged breakwater, and mean water level differences, the research on the velocity of currents near the coastal bed should be examined further in order to supply valid proof for the results since the strength of the current is highly important for sediment transport. Furthermore, the vortexes generated in the newly introduced submerged breakwater are assumed to decrease the transmitted wave power without causing the mean water level to rise. However, its mechanism has not been revealed in this research. In order to further clarify this, the research on vortexes is considered to be needed. Moreover, the two dimensional calculations cannot account for the horizontal flow along the coastal line, thus the changes in mean water level in reality is not considered to be different from the simulated values. Further examinations taking three dimensions into consideration are necessary for. However, the result surely showed a great promise for the future.

Appendix A Incident Waves

In the calibration of $S(f)$, the correction values multiplied by the values given by the Bretschneider-Mitsuyasu spectrum proposed by Goda are repeatedly used (See the equation A.1). When the target spectrum is given by $S_c(f)$ and the spectrum analyzed by CADMAS-SURF is defined as $S_c^{(1)}(f)$, $S_c(f)/S_c^{(1)}(f)$ is used for the correction values. In the next calibration, $(S_c(f)/S_c^{(1)}(f)) \times (S_c(f)/S_c^{(2)}(f))$ is used.

Figure A.1-A.3 below shows the wave spectrum before calibration, after the first calibration and the second calibration, respectively.

A.1 Spectrum of Bretschneider-Mitsuyasu modified by Goda

$$S(f) = 0.205 H_{1/3}^2 T_{1/3}^{-4} f^{-5} \exp\left[-0.75\left(T_{1/3} f\right)^{-4}\right] \quad \text{(Eq. A.1)}$$

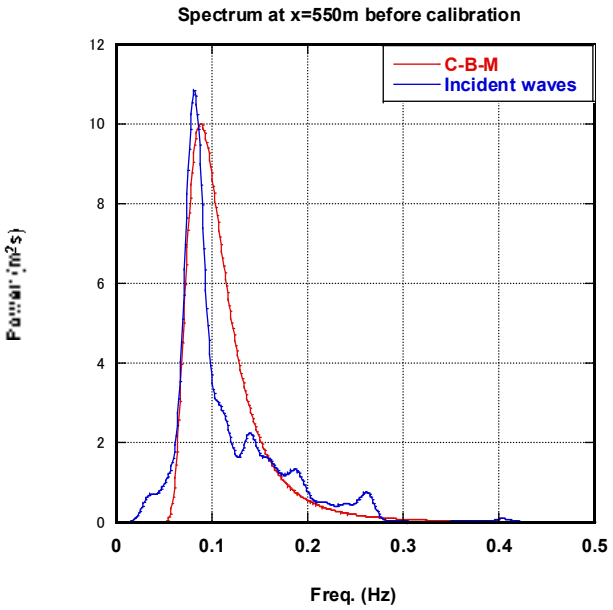

Figure A.1. Wave spectrum of incident waves before calibrations

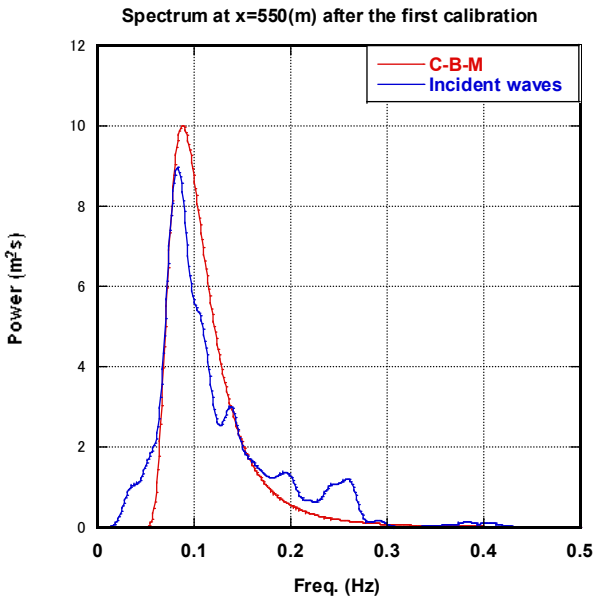

Figure A.2. Wave spectrum after the first calibration

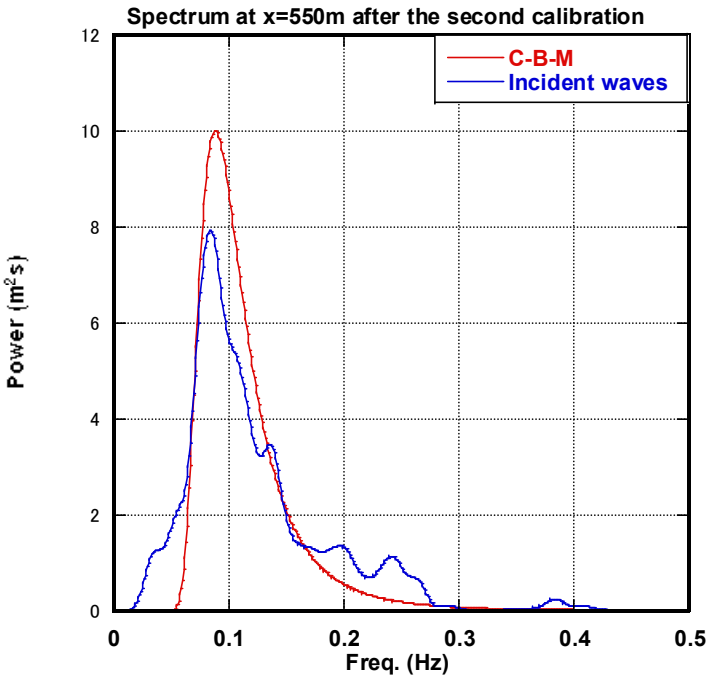

Figure A.3. Wave spectrum after the second calibration

Appendix B Results of All Cases

Appendix B shows the obtained results of all cases, some of which shown in Chapter 4 because they did not give as efficient results as the cases that were presented there. Nevertheless it might be useful to know cases with non-efficient results for future studies, as the loss of time carrying out similar calculations can be avoided, and aspects which I have not realized could be discovered and help to further develop the research.
This is how research should be. The definition of each breakwater given in this appendix might not be explained in greater detail, however, it should be easily understood by reading through Chapter 4.

B-1. Comparison of the trapezoidal submerged breakwaters

In this section, the effect of changing the bank width and height of a submerged breakwater is discussed. The lengths of crest width B_1 and base widths B_2 of Cases A'2.0, A'2.5 and B2.0 are set the same, but the freeboards are different (e=-3.0m, -2.5m and -2.0m. Refer to table 3-1 in Chapter 3 for the bank shapes in each case). Case A' with the same freeboard as Case A (e=-1.5m) was not carried out. This is because the past research has already shown the wider the width is set, the higher the mean water level rise becomes. This means that a wider breakwater with the same freeboard can reduce the transmitted wave power, but will increase the mean water level rise. This is not the objective of this research. Figure B.1.1 and B.1.2 show the wave spectrum at x=700m and mean water level in Case A, A'3.0, A'2.5 and A'2.0 respectively. From the viewpoint of reducing mean water level rise, i.e. from the results in Figure B.1.1.2, Case A'3.0, 2.5 and 2.0 give the better results than Case A. However, from Figure B.1.2, the power of transmitted waves in Case A'3.0 and 2.5 are higher than Case A at any frequency level, and it is found that only Case A'2.0 can reduce the power of transmitted waves as much as Case A, which concludes Case A'3.0 and 2.5 do not have enough bank height to reduce the power of incident waves.

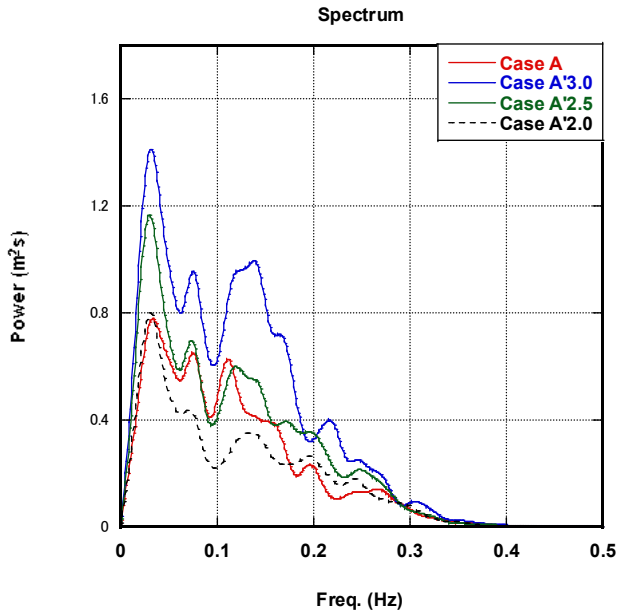

Figure B.1.1 Wave spectrum at x=700m in Case A, A'3.0, A'2.5 and A'2.0

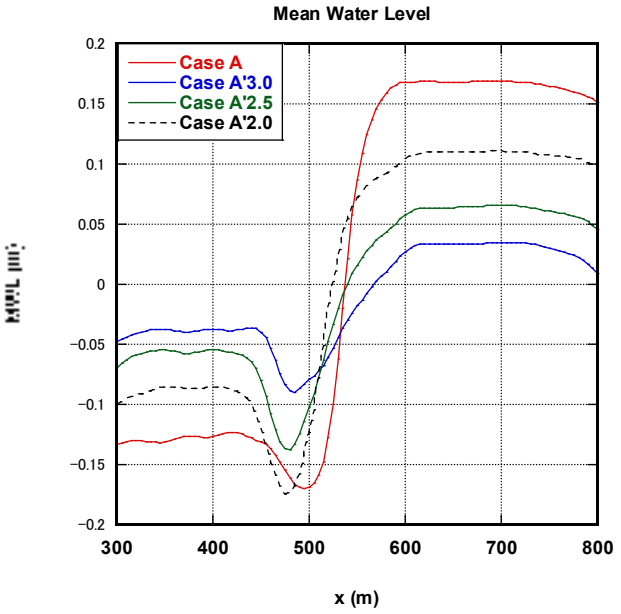

Figure B.1.2 Mean water level in in Case A, A'3.0, A'2.5 and A'2.0

B-2. Comparison of the submerged breakwaters with and without vertical plates at the same structure heights

When comparing the effect of vertical plates, Case B' 2.0 (n=9) shown in Chapter 4-1 was carried out first. And that gave us a good result. However, it is considered to be better if Case B with narrower width or lower plate heights also meet the criteria which can reduce both of the transmitted wave power and mean water level rise, because it can be constructed with smaller amount of constructing materials and it also might have a merit for small in the point capable to pass over such a low submerged breakwater. For that purpose, the cases of n=5, 7, 9 and e=-2.0, -2.5, -3.0 were undertaken. Figure B.2.1-B.2.6 show the results. Case B (e=-3.0) did not minimize the power of transmitted waves as same as Case A, which means higher e=-3.0 is not enough to reduce it (See the Figure B.2.1). Then, the same trial was carried out for Case B (e=-2.5). From Figure B.2.4, it is found that there is no large difference in mean water level between Case A' and Case B. However, looking at Figure B.2.3, Case B allows a larger wave power to pass over the banks in comparison to Case A, this is especially notable with a frequency of 0.1Hz-0.2Hz although they have a large effect of attenuation for the lower frequency band. Therefore, I tried the submerged bank with e=-2.0 in the end. Figure B.2.5 shows that n=7 and n=9 have a larger attenuation effect than Case A and Figure B.2.6 shows mean water level rises that are less that Case A. Therefore, both Case B (n=7) and Case B (n=9) can be considered the better submerged bank than Niigata in both attenuating wave power and minimizing high water level rise.

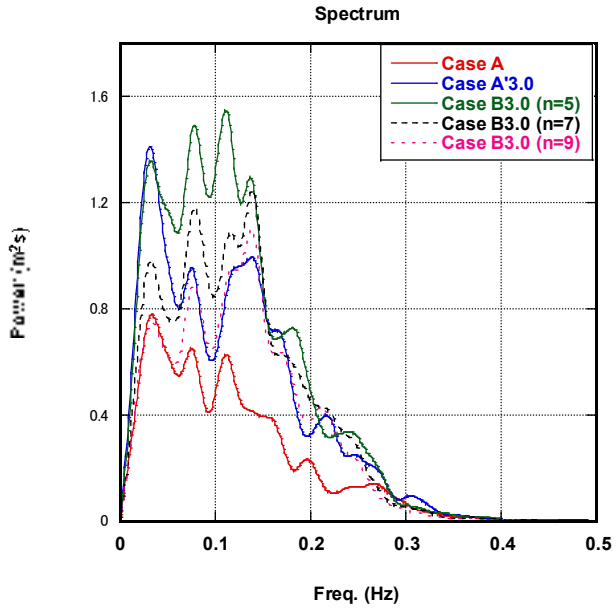

Figure B.2.1 Wave spectrum at x=700m in Case A, A'3.0 and B3.0 (n=5, 7 and 9)

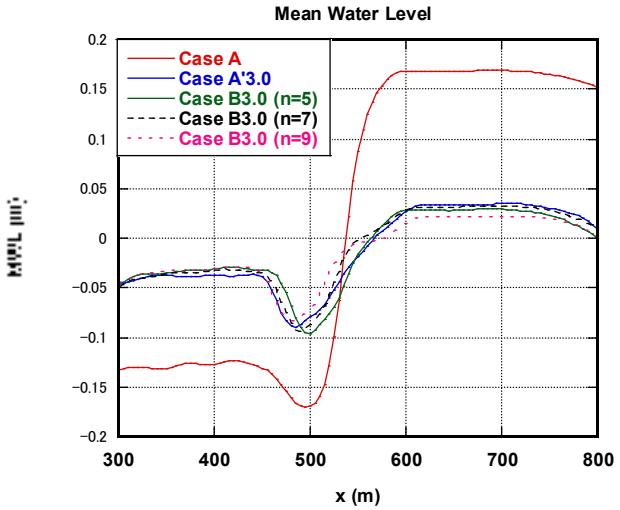

Figure B.2.2 Mean water level in in Case A, A'3.0 and B3.0 (n=5, 7 and 9)

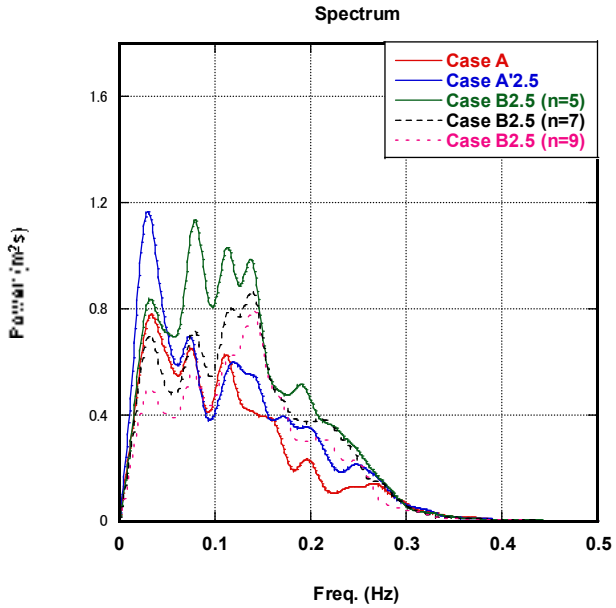

Figure B.2.3 Wave spectrum at x=700m in Case A, A'2.5 and B2.5 (n=5, 7 and 9)

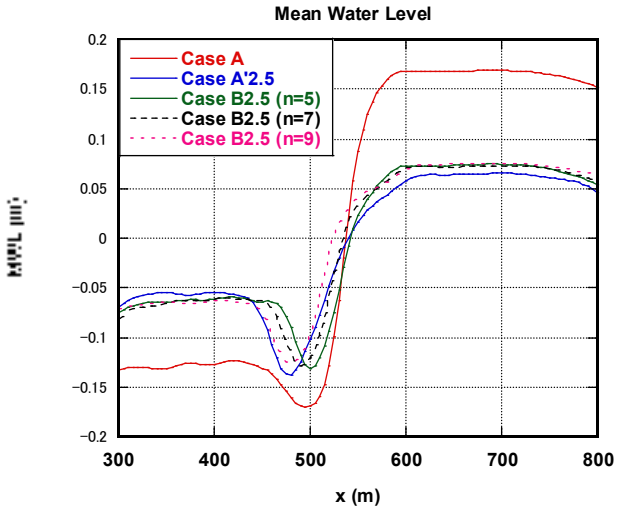

Figure B.2.4 Mean water level in in Case A, A'3.0 and B3.0 (n=5, 7 and 9)

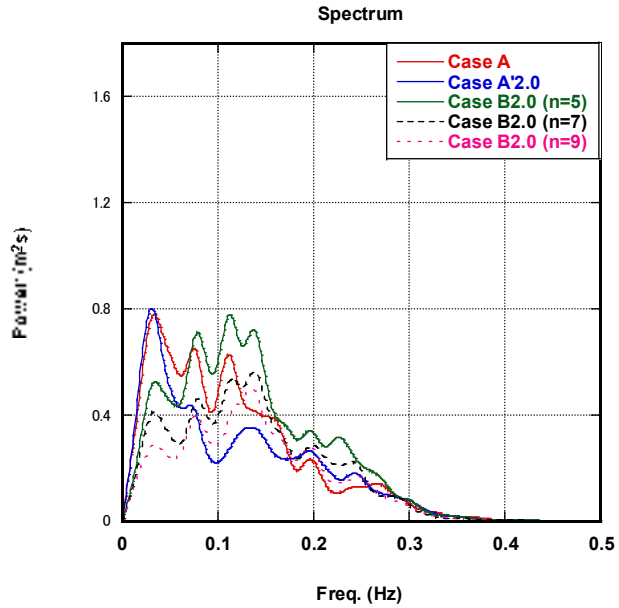

Figure B.2.5 Wave spectrum at x=700m in in Case A, A'2.0 and B2.0 (n=5, 7 and 9)

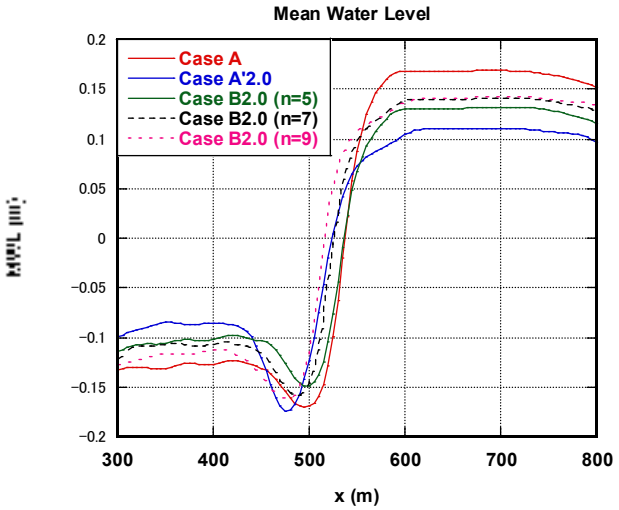

Figure B.2.6 Mean water level in in Case A, A'2.0 and B2.0 (n=5, 7 and 9)

B-3. The effect of vertical plates of two different heights

The sections so far have focused on results obtained by changing freeboard, width, and setting impermeable vertical plates and we could observe that CaseA'2.0, Case B2.0 (n=7) and (n=9) gave better results than Case A. In this section, we will focus on how much effect a bank with two different plate heights has. The objective of this study was to examine the effects when changing the shapes of the trapezoidal breakwater, and it was decided that only the cases with n=9 were to be calculated. Figure B.3.1 and B.3.2 focus on Case C3.0 (See Chapter 3 for the bank shapes in each case). The result was compared with Case A, B3.0 and 2.5 because its height in the offshore were the same as Case B3.0 and one in the onshore side is same as Case B2.5. As a result, it has been shown that Case C3.0 was better than Case B2.5 and 3.0 from the view point of mean water level rise, but it does not seem to have a larger effect on wave attenuation than Case A. Next, Figure B.3.3 and 3.4 focus on Case C2.5, which gave us better results than Case A, B2.5 and B2.0. Finally, Case C 2.5 and C 2.0 are drawn in the same figure in order for the readers to be able to look at the differences between Case C2.5 and C2.0 at one glimpse (See Figure B.3.5 and B3.6).

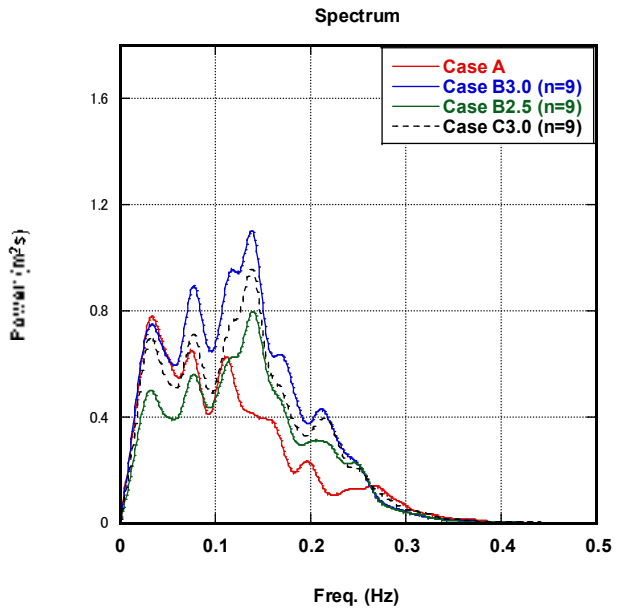

Figure B.3.1 Wave spectrum at x=700m in in Case A, B3.0 B2.5 and C3.0

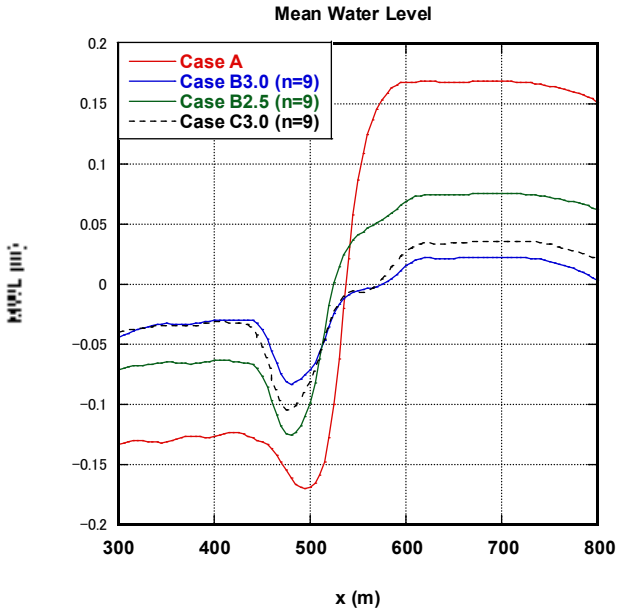

Figure B.3.2 Mean water level in in Case A, A'2.0 and B2.0(n=5, 7 and 9)

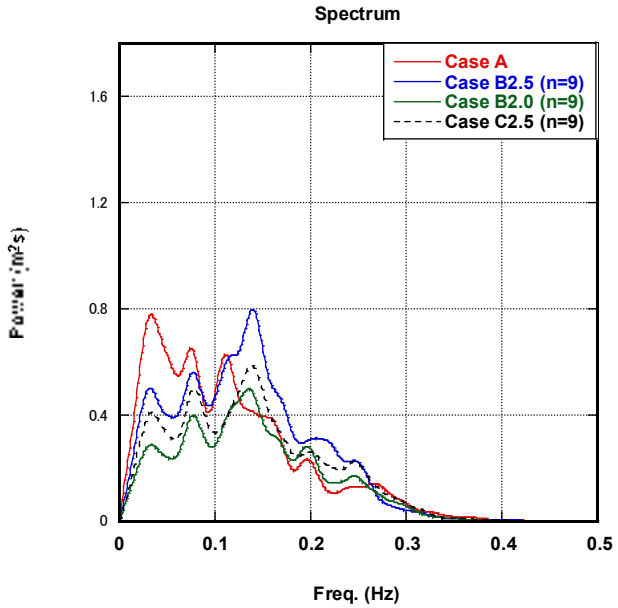

Figure B.3.3 Wave spectrum at x=700m in in Case A, B2.5, B2.0 and C2.5

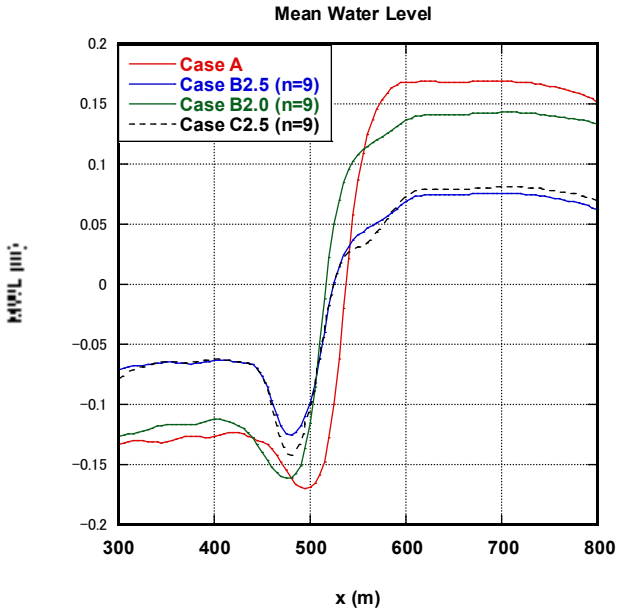

Figure B.3.4 Mean water level in Case A, B2.5, B2.0 and C2.5

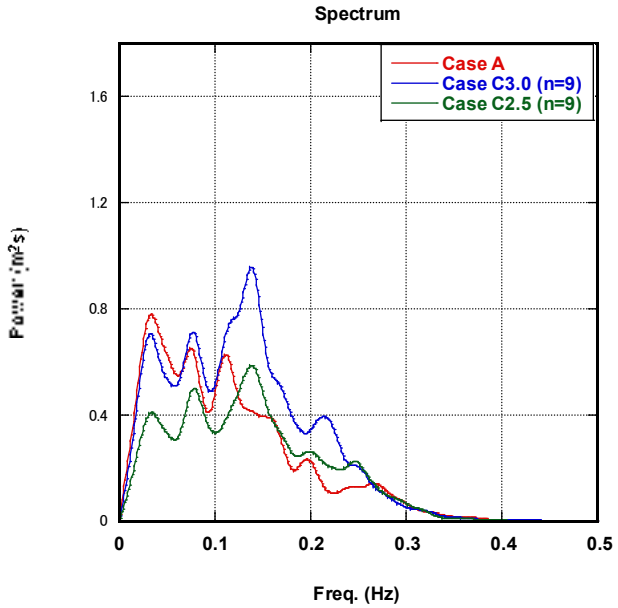

Figure B.3.5 in Wave Spectrum in Case A, C3.0 and C2.5

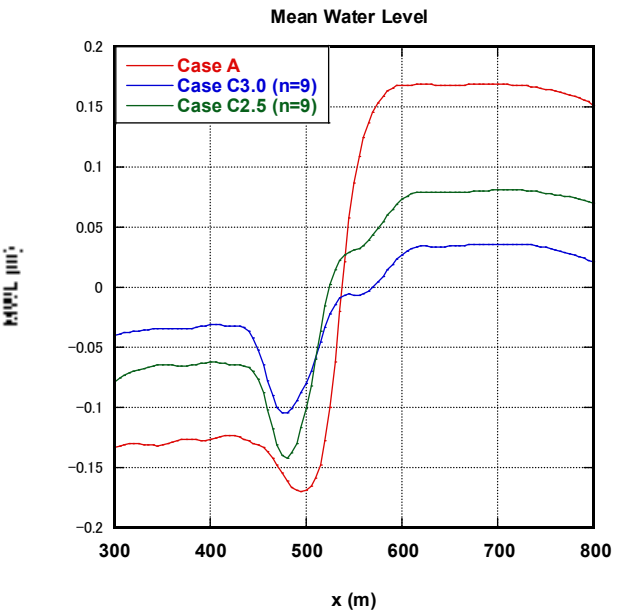

Figure B.3.6 Mean water level in Case A, C3.0 and C2.5

B-4. The effects of vertical plates of three different heights

In Chapter 3, only the results of Case B and Case D were compared because they were enough to know the trend of differences in mean water level rise and wave spectrum of transmitted waves. In this section, Case C was compared to Case D. The Cases compared here were Case C 3.0 and 2.5, and Case D 3.0. Figure B.4.1 shows Case D 3.0 has almost same ability to reduce the power of transmitted waves as Case 2.5. However, Figure B.4.2 shows Case 2.5 allows the mean water level to rise much more than Case D 3.0. This shows it may be more effective to change heights of vertical plates more gradually.

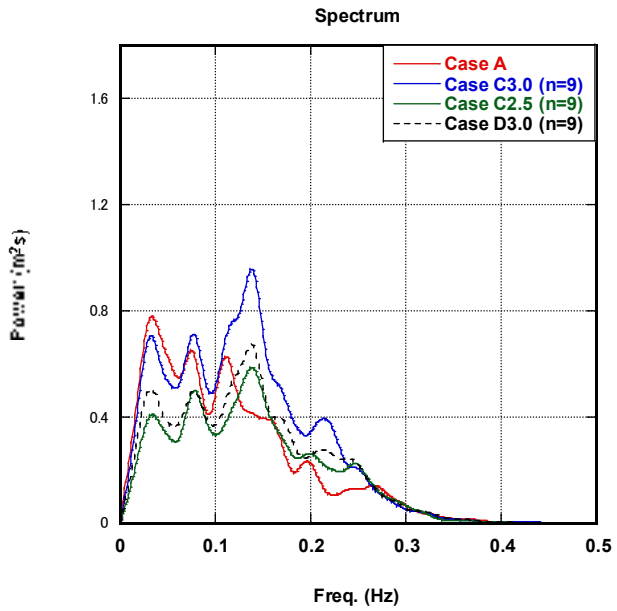

Figure B4.1. Wave spectrum in Case A, C3.0, C2.5 and D3.0

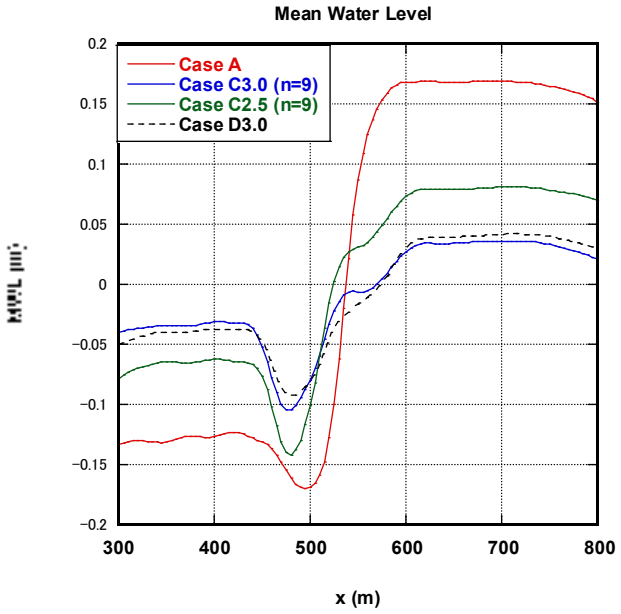

Figure B4.2 Mean water level in Case A, C3.0, C2.5 and D3.0

B-5. The effects of wave shoring in Case A, A' and D

In chapter 4, the results of spectrum Analysis at the water depth of 8.0m and 4.0m (on the slope) were given. These numbers were sufficient for understanding the character in wave shoaling, however, as the results for how the wave spectrum changes along a slope could be of interest for future research, it will be shown in this section where I will present the wave spectrum at x=700m, 720m, 740m, 760m, 780m and 800m, where h=8m, 7m, 6m, 5m, 4m and 3m, in the following Figure B.5.1-B.5.6.

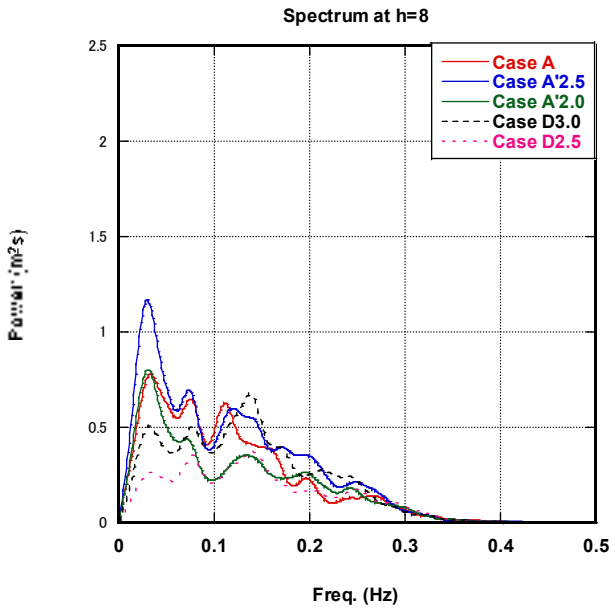

Figure B.5.1 Spectrum Analysis at X=700m

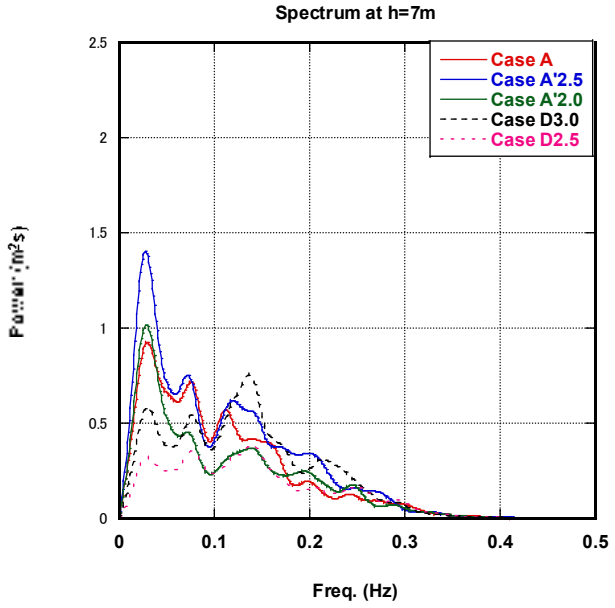

Figure B.5.2 Spectrum Analysis at X=720m

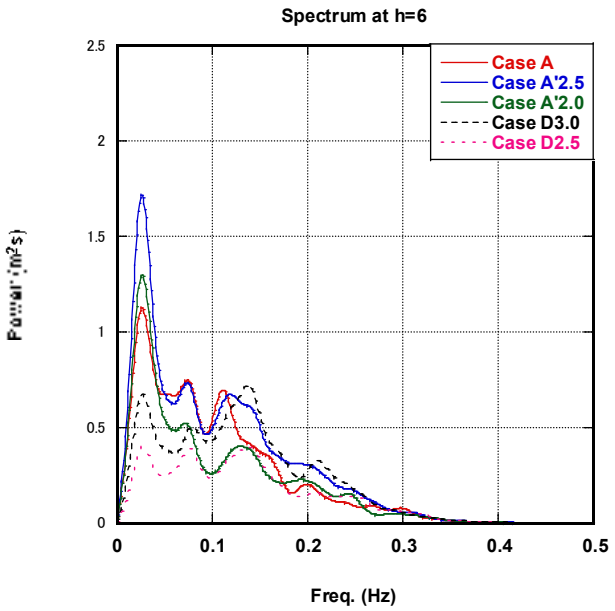

Figure B.5.3 Spectrum Analysis at X=740m

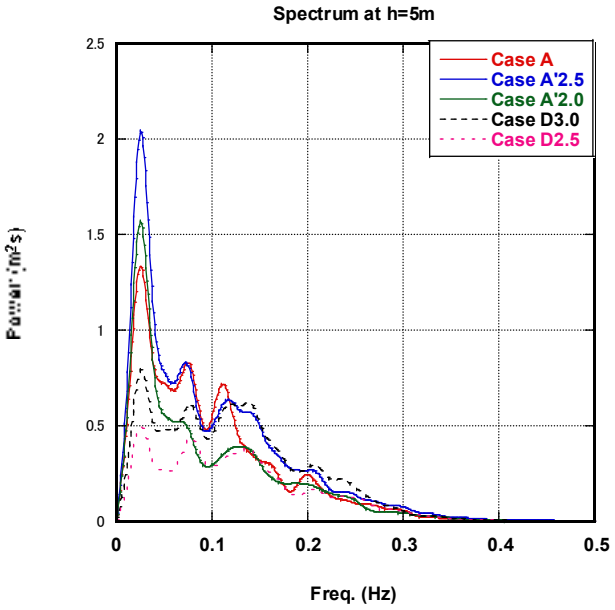

Figure B.5.4 Spectrum Analysis at X=760m

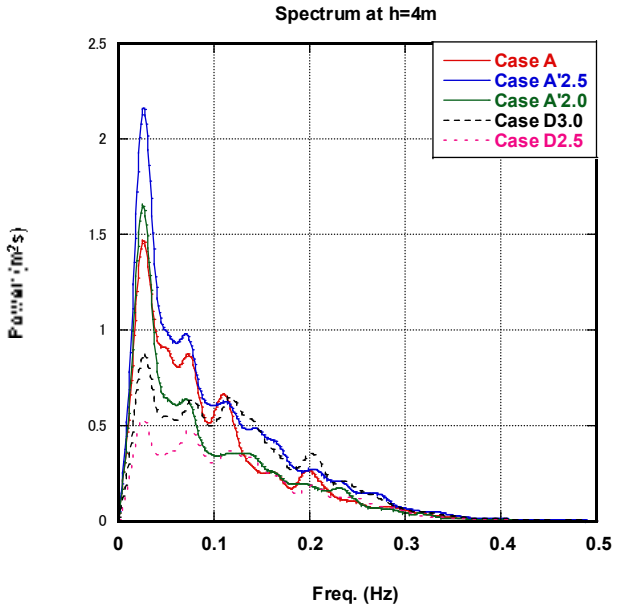

Figure B.5.5 Spectrum Analysis at X=780m

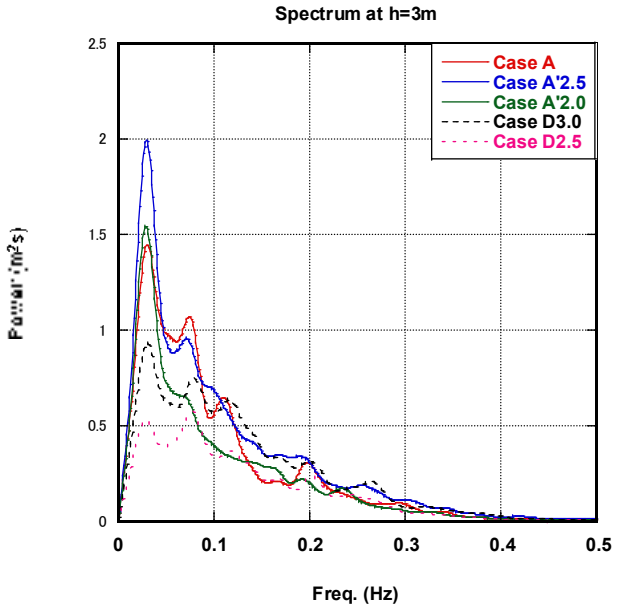

Figure B.5.6 Spectrum Analysis at X=800m

B-6. Wave velocity

The velocity distribution in Case A and D at certain times were given in Chapter 4. The velocity distribution at every one second for one period are given here ($T_{1/3}$=10s, so 10 for each case).

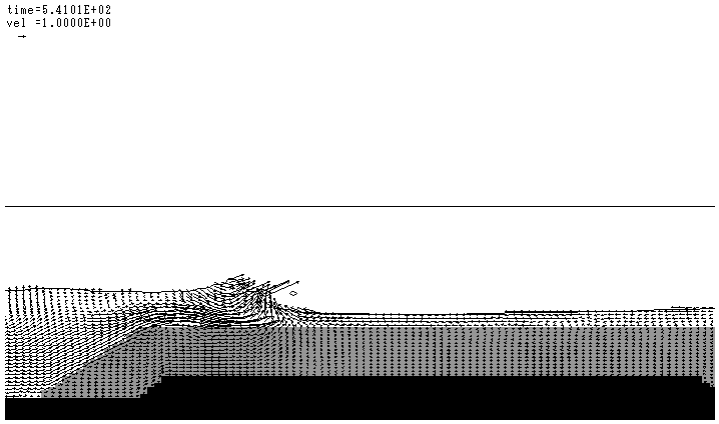

Figure B.6.1 Wave velocity distribution in Case A (t/T=1/10)

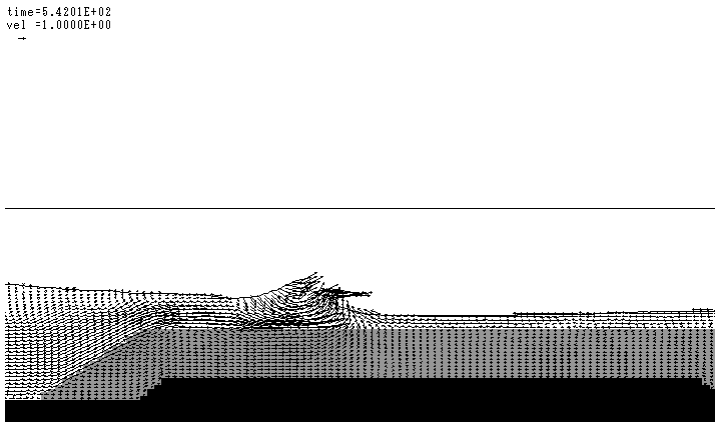

Figure B.6.2 Wave velocity distribution in Case A (t/T=2/10)

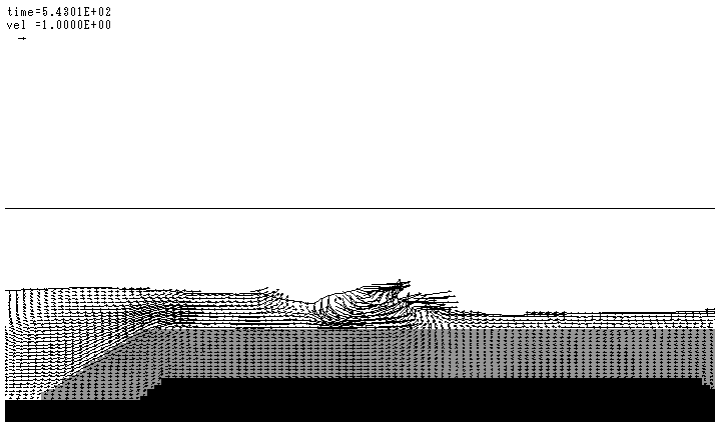

Figure B.6.3 Wave velocity distribution in Case A (t/T=3/10)

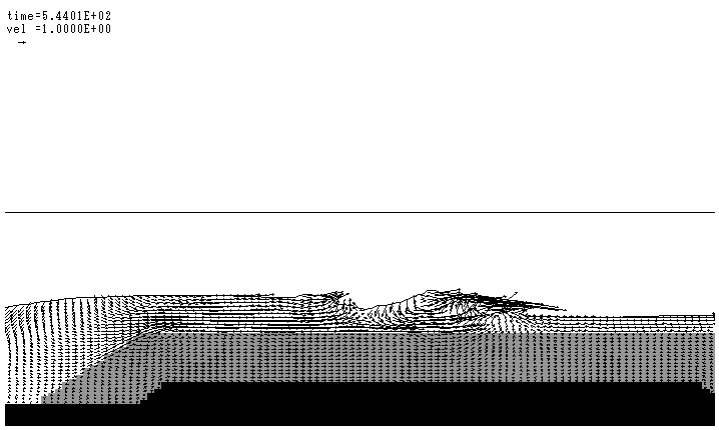

Figure B.6.4 Wave velocity distribution in Case A (t/T=4/10)

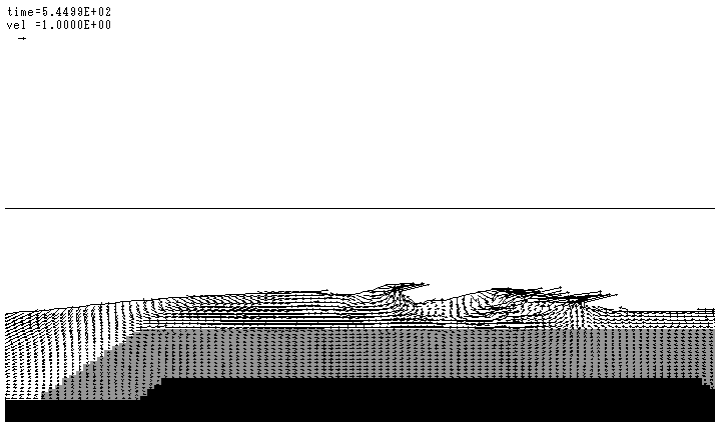

Figure B.6.5 Wave velocity distribution in Case A (t/T=5/10)

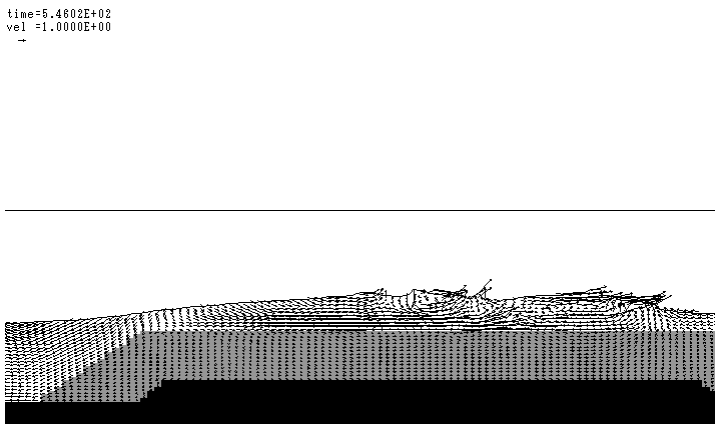

Figure B.6.6 Wave velocity distribution in Case A (t/T=6/10)

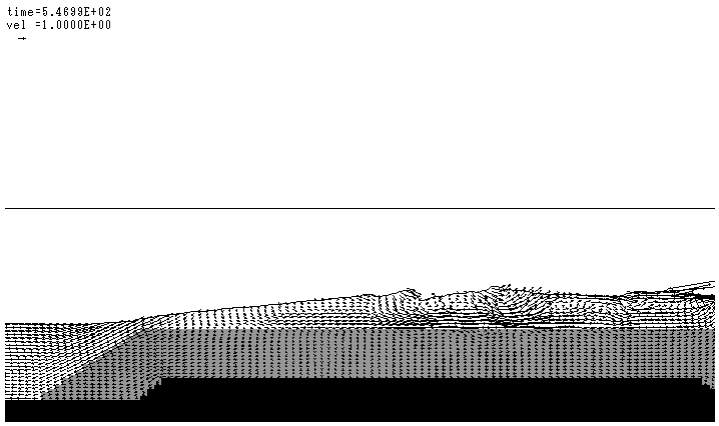

Figure B.6.7 Wave velocity distribution in Case A (t/T=7/10)

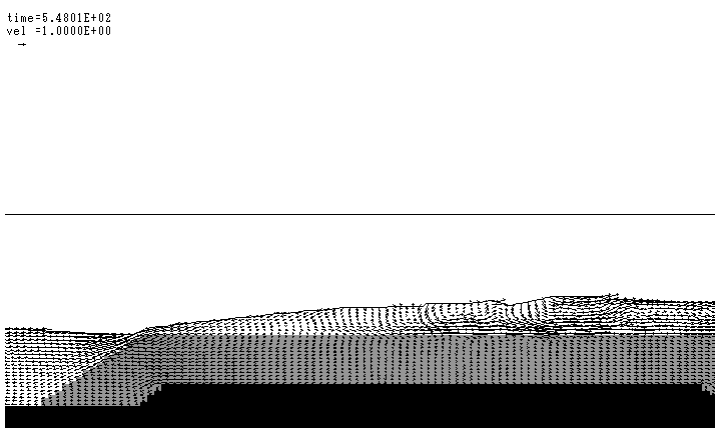

Figure B.6.8 Wave velocity distribution in Case A (t/T=8/10)

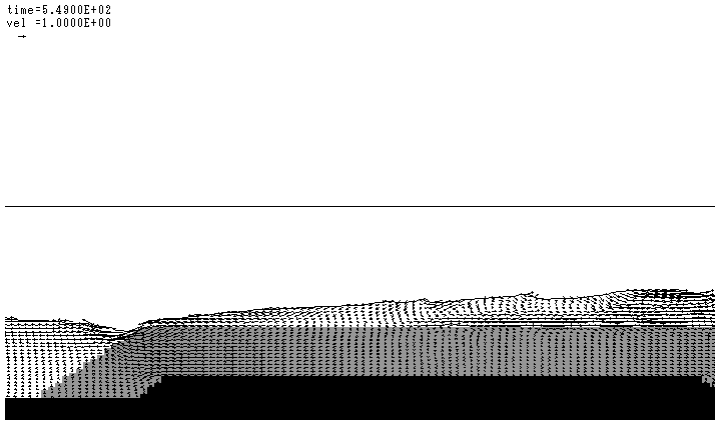

Figure B.6.9 Wave velocity distribution in Case A (t/T=9/10)

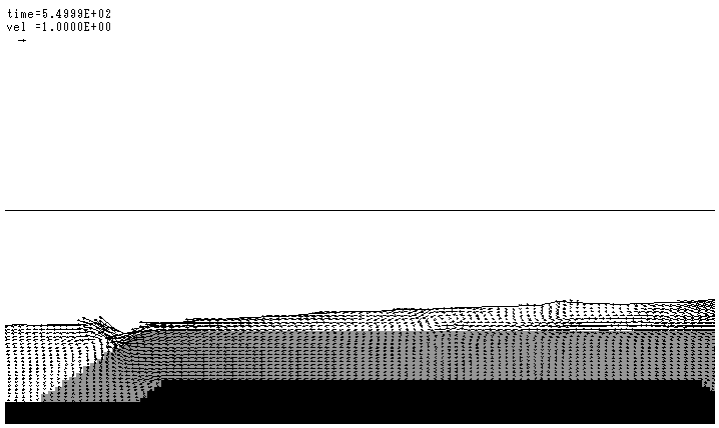

Figure B.6.10 Wave velocity distribution in Case A (t/T=10/10)

Fluid velocity for one period in Case D: Submerged breakwater with vertical plates of different heights

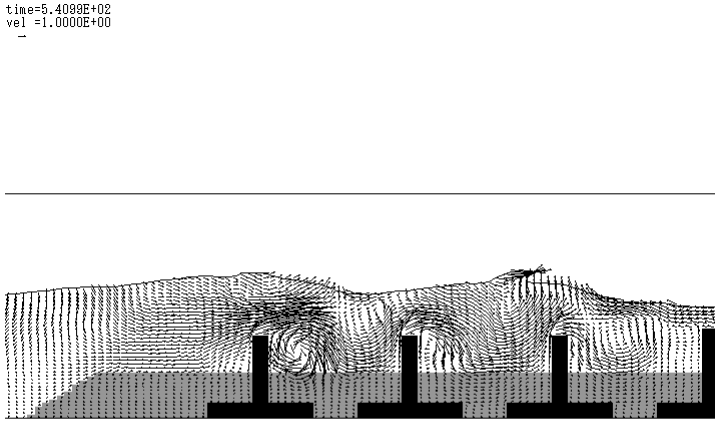

Figure D.6.11. Wave velocity distribution in Case D (Newly-introduced submerged bank) t/T=1/10

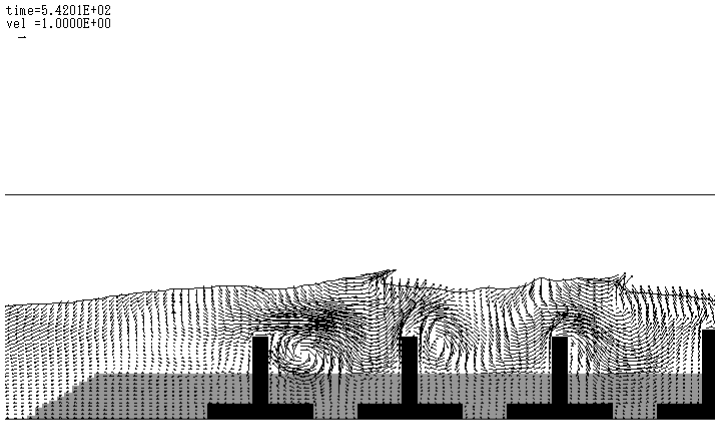

Figure B.6.12 Wave velocity distribution in Case D (Newly-introduced submerged bank) t/T=2/10

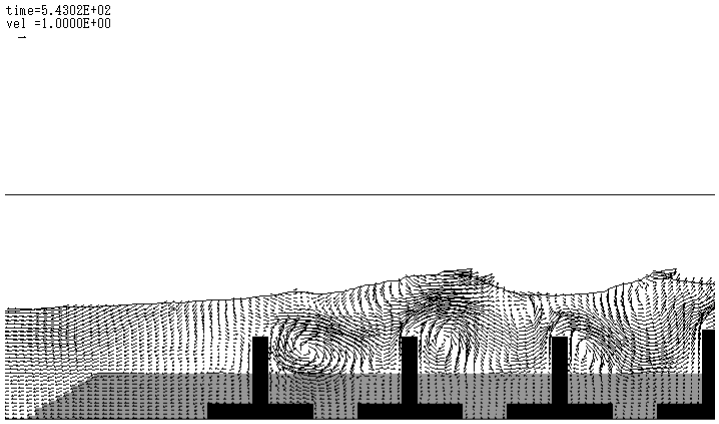

Figure B.6.13 Wave velocity distribution in Case D (Newly-introduced submerged bank) t/T=3/10

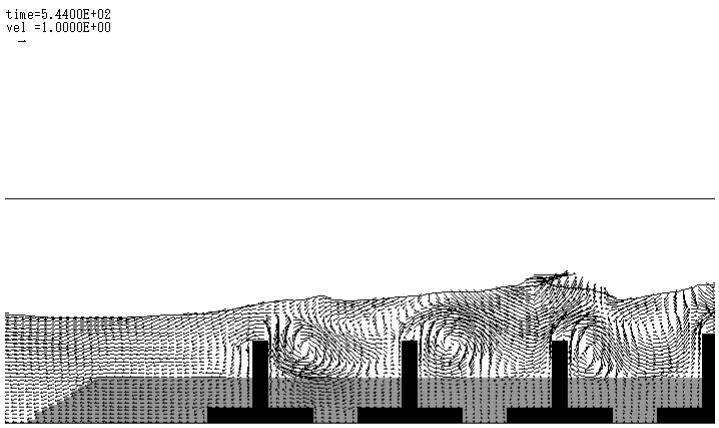

Figure B.6.14 Wave velocity distribution in Case D (Newly-introduced submerged bank) t/T=4/10

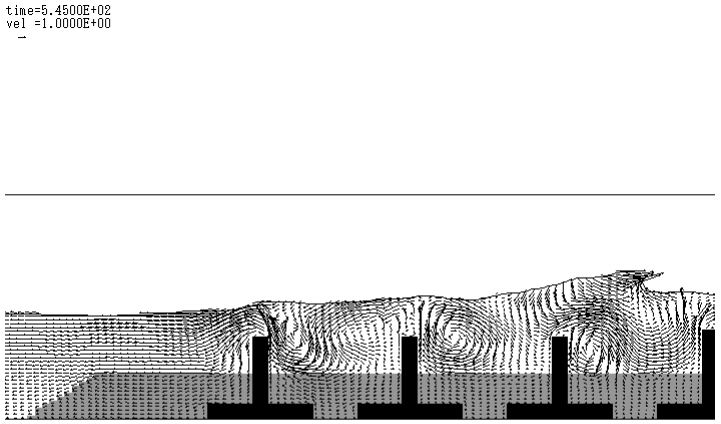

Figure B.6.15 Wave velocity distribution in Case D (Newly-introduced submerged bank) t/T=5/10

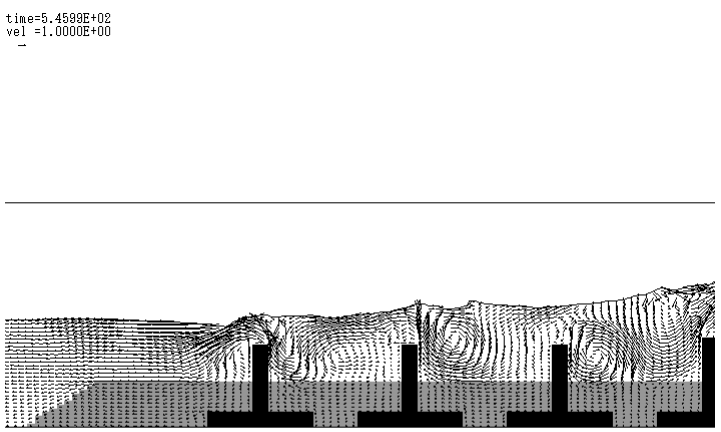

Figure B.6.16 Wave velocity distribution in Case D (Newly-introduced submerged bank) t/T=6/10

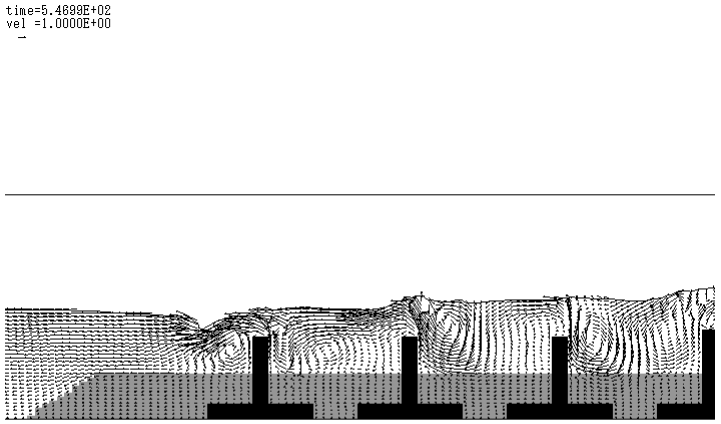

Figure B.6.17 Wave velocity distribution in Case D (Newly-introduced submerged bank) t/T=7/10

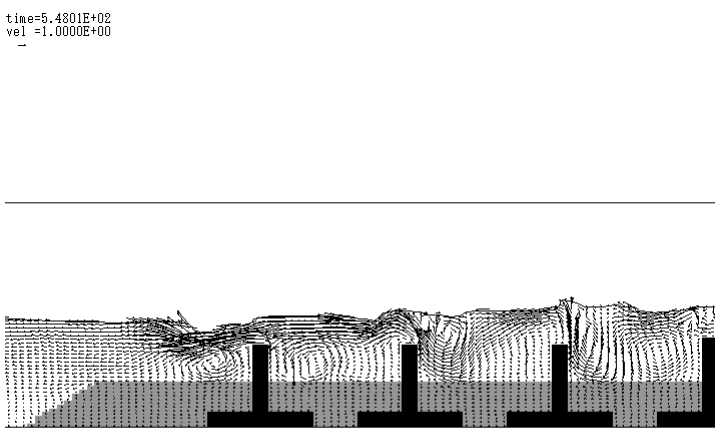

Figure B.6.18 Wave velocity distribution in Case D (Newly-introduced submerged bank) t/T=8/10

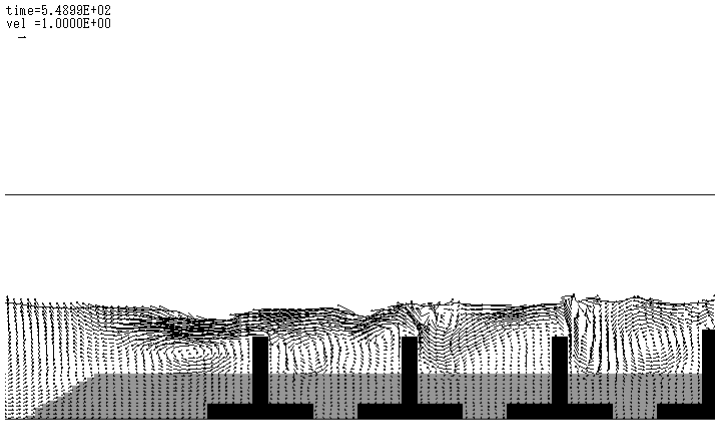

Figure B.6.19 Wave velocity distribution in Case D (Newly-introduced submerged bank) t/T=9/10

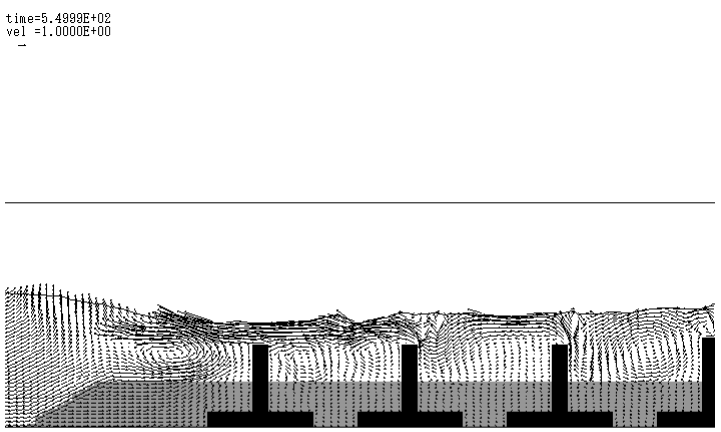

Figure B.6.20 Wave velocity distribution in Case D (Newly-introduced submerged bank) t/T=10/10

6. References

- Calabrese, M., Vicinanza, D.,and Buccino, M., (2003). 2D Wave Set Up behind Low Crested and Submerged Breakwaters. The International Society of Offshore and Polar Engineers, Vo.3, p831-836

- Coastal Development Institute of Technology, Japan (2012) Handouts in the technical community in the west coast of Niigata (in Japanese)

- Coastal Development Institute of Technology, Japan (2001). CADMAS-SURF, Development for the numerical simulation of waves. CDIT library, Vol.12, 5-29 (in Japanese)

- Fernando J. Me´ndez, J. Losada, Inigo, and Miguel A. Losada, (2001). Wave-induced mean magnitudes in permeable submerged breakwaters, Journal of waterway, port, coastal, and engineering, p7-15

- Hirt, C.W., and Nicholos, B.D., (1981), Volume of Fluid (VOF) Method for the Dynamics of Free Boundaries. Journal of computational physics 39, p201-225

- Kuriyama, Y., Yamaguchi, S., Ikegami, M., Takano, S., and Tanaka, J.,(2006). Morphological changes around large-scale submerged breakwaters on the Niigata coast, Japan. Coastal engineering, Vol.4, p3694-3707.

- Loveless, J. H., and Debski, D., (1998). Sea level set-up behind detached breakwaters. Coastal engineering, p1665-1678

- Ministry of Land, Infrastructure, Transport and Tourism (2001). Pamphlet for the west coast of Niigata (in Japanese)

- Nakagawa, Y., Oshita, Y., Yamakawa, K., Hasegawa, I., and Inagaki, S., (2011) Experimental study on submerged breakwater and end section of large-scale shore

protection facility. Journal of JSCE, Vol. 67 No. 2 pp.I_70-I_75

- Phung Dang Hieu, Katsutoshi Tanimoto, (2006) Verification of a VOF-based two-phase flow model for wave breaking and wave–structure interactions, Ocean Engineering 3, p1565–1588

- Pilarczyk, K. W. and Zeidler, R. B., (1996). Offshore Breakwaters and shore evolution control. A.A.Balkema publishers, Rotterdam. p183-184

- The Coastal Engineering Research Center of the U.S. Army Engineer Waterways Experiment Station, (1984), Shore Protection Manual. US Army Corps of Engineers, Washington DC, 2-17.

- The overseas coastal area development institute of Japan, (2002) Technical standards and commentaries for port and harbour facilities in Japan. The overseas coastal area development institute of Japan, Tokyo, p38-40

- Yoshida, A., Kisanuki, T., Koga, S., and Kojima, H.,(1988) Reflexion of Water Waves by a “Submerged-Double-Plate-Breakwater”, Technology Reports of Kyushu University Vol.61, No.2, p103-110 (in Japanese)

Acknowledgements

I spent my student life as the first student of a Double Degree program at Kyushu and Lund University. Although I sometimes met with difficulties, I would say that my life was full of happiness and I was able to experience such a splendid school life because a lot of people always helped me.

First, I would like to express my appreciation towards my supervisor, Associate Professor Akinori Yoshida of Kyushu University, for his very helpful instructions in the process of writing my thesis. I will also never forget how he cared for me even while I was studying abroad, which helped me to study at ease. Furthermore, I owe a substantial debt to Assistant Professor Masaru Yamashiro of Kyushu University, for his help with my research. Thanks to him, I managed to finish my study in the end. I also would like to express my gratitude to Professor Noriaki Hashimoto of Kyushu University, Assistant Professor Masaki Yokota of Kyushu University, and technical officer Mitsuyoshi Kodama of Kyushu University for their useful advice. I owe another great debt to Professor Koichiro Watanabe of Kyushu University and ITP Office of Kyushu University, who gave me the opportunity to go study abroad.

My deepest appreciation also goes to Professor Magnus Larson of Lund University, Professor Hans Hansson of Lund University and Professor Ronny Berndtsson of Lund University. They not only assisted me in developing academically, but also cared for me during my stay in Lund, and in the beginning of my life in Lund, often asked me if all was well. I also wish to thank Christina Grossman of the International Office, Lund University. Every time I met with difficulties in my studies, she offered fabulous instruction.

I also want to thank my friends at Kyushu and Lund University. Without them, my student life would not have been such a splendid experience.

Finally, I would like to express my gratitude to my dear family for all their long-time support.
My humblest thanks to you all.